Methods for Calculating Motion Induced Interruptions as Applied to a Space Capsule After Splashdown

Lauren W. Hanyok

Thesis submitted to the Faculty of the
Virginia Polytechnic Institute and State University
in partial fulfillment of the requirements for the degree of

Master of Science
in
Ocean Engineering

Leigh S. McCue-Weil, Chair
Alan J. Brown
William F. Belknap

November 13, 2012
Blacksburg, Virginia

Keywords: motion induced interruptions, unique hull form, space capsule, accelerations, human factors

Methods for Calculating Motion Induced Interruptions as Applied to a Space Capsule After Splashdown

Lauren W. Hanyok

ABSTRACT

The introduction of calculation methods for motion induced interruptions (MII) in 1984 introduced a new way to quantify human factors in addition to the motion sickness index (MSI). The 1990 Graham method for calculating MII uses a combination of a vessel's acceleration and roll to determine a "tipping" factor to calculate MII per minute. The Applebee-Baitis (AB) method considered that the motions are implicitly considered in accelerations, and therefore did not require roll to calculate MII. This thesis examines and analyzes the differences between the AB and Graham methods and compares their results for a unique hull form shape, a cylindrical capsule, in rough seas to determine which method is preferred. A one-quarter test was performed by the Naval Surface Warfare Center, Carderock Division (NSWCCD) for the National Aeronautics and Space Administration (NASA) on the Orion Crew Exploration Vehicle (CEV) in post-splashdown conditions at the Aberdeen Test Center in Aberdeen, Maryland. Direct comparison of the analyzed data, MII sensitivity to location, and scaling analyses are examined and future work to further the application of MII calculation methods are proposed. The symmetry of the capsule leads to the assumption that roll and pitch-dominant MII calculations should be on the same order of magnitude. They are not because both MII methods only take roll-motions into account. The inclusion of both pitch and roll motions for the MII calculations is proposed as future work. The Graham method was found to be the more appropriate calculation because it is more conservative, and therefore preferred in the context of crew safety.

Acknowledgments

This work was supported in part by the Naval Surface Warfare Center, Carderock Division (NSWCCD), and by the National Aeronautics and Space Administration (NASA). Thank you to the NASA Orion personnel, particularly **Mr. Alan Rhodes** for his support during testing and of this thesis. The research and work performed to provide the foundation for thesis can be found in Chapters 1, 2, and 3. All figures used with permission.

I would like to express my appreciation and thanks to all the people who helped make this thesis a reality:

Dr. Leigh McCue-Weil, committee chairman, for taking me on as one of her "virtual" graduate students, for all her help during my graduate studies, her patience with my persistent questions in the classes she taught, and her constant motivation to help me realize my full potential.

Dr. Alan Brown and **Dr. William Belknap**, committee members, for their support and helpful feedback during this process.

Mr. Chris Bassler, NSWCCD co-worker, for providing funding through Dr. John Barkyoumb and the Naval Innovative Science and Engineering Program at NSWCCD, for his endless support during his own doctoral thesis work, for always giving constructive criticism to help me improve my critical thinking and writing skills, for keeping me sane at work, and for believing that I can do anything I put my mind to.

Mr. Todd Carrico, former NSWCCD co-worker, for his guidance, constant support and encouragement academically and professionally, for inspiring me to work towards his level of engineering excellence and hard work, for providing the opportunity to work with him on the projects upon which this thesis was derived, and for good-naturedly putting up with my tendency to drop by his office to talk about (mostly) Star Wars and Battlestar Galactica, despite his busy schedule.

Mr. Terrence Applebee, former NSWCCD supervisor, for the opportunity to continue my education through the Navy, for his constant support and encouragement academically

and professionally, for his enthusiastic support in my interest of Human Factors and allowing me to join this small, yet strong, professional community, for his guidance on the Applebee-Baitis Method, of which he is a co-creator, and full support in using it in this thesis.

Mr. Martin Dipper, NSWCCD supervisor, for his support throughout my graduate studies, for his constant encouragement and constructive feedback academically and professionally, for making time to talk with me about science fiction and the future of technology, despite his busy schedule, for pushing me outside my comfort zone professionally, and investing in my professional future.

Mr. Matt Powell, NSWCCD co-worker, for keeping up with and providing me with the Applebee-Baitis method program, the only known documentation of the method in full, and his guidance on its theory and use.

Ms. Lisa Minnick, NSWCCD co-worker, for her constant support and willingness to answer all my questions about the writing, presentation, and finalization of a thesis.

Non-committee member **readers and editors** of this thesis, who graciously agreed to do so without reservations: **Mr. Ryan Hanyok, Mrs. Sue Watson, Mr. Mike Watson, Mr. Paul Muessig, Mrs. Erin Muessig, Mr. Ray Chattman, Mrs. Kathy Hanyok, Mr. Mike Renner, Ms. Diana McMillion, Mrs. Trisha Shields, Mr. Chris Bassler,** and **Mr. Alan Rhodes**, for their helpful suggestions and feedback that were essential to helping me communicate my thoughts, results, and conclusions into something readable.

All my friends who have been nothing but supportive; especially to **The Council: Mrs. Trisha Shields, Mr. Eric Shields, Mr. Mike Renner, Ms. Diana McMillion, Mr. Brendan Mulhare, Mr. Paul Muessig, and Mrs. Erin Muessig**, with special thanks to **Trisha**, my best friend, for empathizing with me as she worked on her own graduate studies, for her crazy humor and intense silliness which kept me moving forward; the members of our basement band **Metallifun**, **Mr. Eric Taylor, Mr. Robbie Taylor**, and **Mr. Ryan Hanyok** for being able to rock out to our favorite heavy metal bands every week, despite their own school and work commitments.

My family, for their constant support and encouragement, especially my sister and brother-in-law, **Mr. and Mrs. Paul Muessig**, my mother-in-law, **Mrs. Kathy Hanyok**, and my brother- and sister-in-law, **Mr. Dan Hanyok** and **Ms. Tate Hanyok**, who were unwaveringly supportive and enthusiastic; all my grandparents, aunts, uncles, and cousins, the **Lusby's, Watson's, Miller's, Hoesten's,** and **Young's**, who did nothing but shower me with moral support and love.

Mr. and Mrs. Mike Watson, my parents for their financial and undying moral support throughout my undergraduate studies at Virginia Tech, which led to my current employment at NSWCCD and subsequent graduate studies; for their constant encouragement for everything I have done and everything I want to do; without their love and support, I could never have gotten this far.

And finally, my husband, **Mr. Ryan Hanyok**, for his constant love and support, for putting up with the ups and downs of work and school, for being silly when I needed it, for rocking out with me at concerts, band practice, and at home to drown out the stress, for keeping me grounded and focused; without his love, support, motivation, and tendency to start playing the music of Metallica, Iron Maiden, Gorod, and Sabaton on his guitar for me while I was writing and researching, this thesis would not have been finished.

Dedication

This thesis is dedicated to the memory of my grandfather, Captain Luther P. Hoesten of the Army Air Corps, who always looked for the chance to learn more and constantly inspired me to strive for amazing things.

"It's a good day for flying." - L.P. Hoesten

Contents

List of Figures

List of Tables

List of Acronyms

AM	abort maximum
APG	Aberdeen Proving Grounds
CEV	Crew Exploration Vehicle
CG	center of gravity
CL	centerline
DOF	degree of freedom
DREA	Defence Research Establishment Atlantic
FB1	forward bay edge 1
FB2	forward bay edge 2
FBD	free-body diagram
FF	fully flooded
FFG	Guided Missile Frigate
GLFE	general lateral force estimator
ISS	International Space Station
LAMPS	Light Airborne Multipurpose System
LFE	lateral force estimator
LM	landed minimum
LMS	Large Motion Simulator
LWE	Littoral Warfare Environment

MII	motion induced interruption
MUV	manned underwater vehicle
NASA	National Air and Space Administration
NATO	North Atlantic Treaty Organization
NATO STANAG	North Atlantic Treaty Organization Standardization Agreement
NSWCCD	Naval Surface Warfare Center, Carderock Division
OGM	Operator guidance Manual
PF	partially flooded
PORT	Post-Landing Orion Recovery Test
RAO	response amplitude operator
RAST	Recovery Assist Secure and Traverse
S1	seat 1 eye point
S2	seat 2 eye point
S3	seat 3 eye point
S4	seat 4 eye point
S5	seat 5 eye point
S6	seat 6 eye point
SH	side hatch bottom
SHIPMO	SHIP MOtions
SS	sea state
TH	top of docking hatch
TPM	tips per minute
VCG	vertical center of gravity

Nomenclature

a	half the length of an ellipsoidal cylinder minor axis
a_1	measured acceleration
a_2	translated acceleration
a_t	transverse acceleration
a_v	vertical acceleration
b	half the length of an ellipsoidal cylinder major axis
C_T	tipping coefficient
$\vec{D}$	displacement
$\dot{\vec{D}}$	velocity
$\ddot{\vec{D}}$	acceleration
$\ddot{D}_1$	longitudinal acceleration
$\ddot{D}_2$	lateral or transverse acceleration
D_{MII}	time taken to recover from an MII (seconds per tip)
D_{TASK}	delay in completing a task
g	acceleration due to gravity
E_{TASK}	task effectiveness
$\vec{F}$	forces acting upon a person's CG
F_{lat}	lateral force per unit mass
F_{long}	longitudinal force per unit mass

F_{vert}	vertical force per unit mass
h	height of a person's VCG
$H_{1/3}$	significant wave height
$\mathbf{I}$	moment of inertia at the CG of a person
l	half-width of a person's stance
m	the mass of a person
M_E	moment due to a ship's rotation in the Earth-reference frame
M_L	moment about the left foot
$M_{L_{total}}$	total moment about the left foot
M_S	moment due to a ship's rotation in the ship-reference frame
MII_{CALM}	MII experienced under calm conditions
MII_{RATE}	motion induced interruptions (tips per minute)
$\vec{O}_L$	vector between the left food and a person's CG
r	position vector
$\dot{r}$	velocity
R_T	tipping ratio
t	time
T_{CALM}	time required to complete a task under calm sea conditions
T_M	modal period
T_{WAVES}	observed time to complete the same task while underway
v	velocity
$\dot{v}$	acceleration
$\vec{\eta}$	translational displacements
$\dot{\vec{\eta}}$	translational velocities
$\ddot{\vec{\eta}}$	translational accelerations
$\vec{\eta}_1$	surge displacement
$\dot{\vec{\eta}}_1$	surge rate
$\ddot{\vec{\eta}}_1$	surge acceleration

$\vec{\eta}_2$	sway displacement
$\dot{\vec{\eta}}_2$	sway rate
$\ddot{\vec{\eta}}_2$	sway acceleration
$\vec{\eta}_3$	heave displacement
$\dot{\vec{\eta}}_3$	heave rate
$\ddot{\vec{\eta}}_3$	heave acceleration
$\vec{\eta}_4$	roll angle
$\dot{\vec{\eta}}_4$	roll rate
$\ddot{\vec{\eta}}_4$	roll acceleration
$\vec{\eta}_5$	pitch angle
$\dot{\vec{\eta}}_5$	pitch rate
$\ddot{\vec{\eta}}_5$	pitch acceleration
$\vec{\eta}_6$	yaw angle
$\dot{\vec{\eta}}_6$	yaw rate
$\ddot{\vec{\eta}}_6$	yaw acceleration
λ	scale ratio
θ	roll angle
$\vec{\xi}$	rotational displacements
$\dot{\vec{\xi}}$	rotational velocities
$\ddot{\vec{\xi}}$	rotational accelerations
ω	angular velocity
$\dot{\omega}$	angular acceleration

Chapter 1

Introduction

This chapter introduces the concept of motion induced interruptions (MII) and gives a brief background of its discovery. Two specific methods for calculating MII are described, including a discussion on task effectiveness and recovery time, the current NATO standard, and past experiments. Finally, the motivation for this thesis and its objectives are defined.

1.1 Background

Motion Induced Interruptions (MII) are defined as incidents where ship motions are large enough to cause a person to lose their balance unless they temporarily abandon their allotted task and adjust themselves to remain upright.[3] When such a tipping event occurs, time is lost during the performance of the task. The calculation of MII allows for the indirect prediction of lost time while in various sea conditions, relative wave headings, and ship

speeds. This can be an important tool when considering crew safety and task effectiveness. The time it takes the human body to recover from a tip can further complicate the problem, adding to the importance of properly calculating MII.

MII are calculated in "tips per minute" (TPM). MII can be defined for multiple task types, including walking toward the forward or aft part of a vessel, walking between port and starboard (also called athwart ships), standing facing forward or aft, standing athwart ships, weapon loading, etc. Two tasks have been identified for analysis of the data presented in this study. Standing facing forward or aft is designated as Task A and standing facing athwart ships is designated as Task B.

The concept of MII was first introduced in 1984 at the Naval Surface Warfare Center, Carderock Division (NSWCCD), in Bethesda, Maryland.[4] A MII analysis was further developed in the time domain a few years later but was never published. It was then adopted into the frequency domain in 1990 and 1992.[2][5] There has since been continued development of the frequency domain method.

1.1.1 Concept

Erich Baitis, Terrence Applebee, and Thomas McNamara introduced the concept of MII in 1984, while developing an extension of the FFG/LAMPS MK III Operator Guidance Manual (OGM). The OGM applied human factors considerations for the deployment of the Light Airborne Multipurpose System (LAMPS) helicopter aboard the FFG-8, a Guided Missile

Frigate class Navy ship.[4].

The authors studied crew tasks involved with the helicopter Recovery Assist Secure and Traverse (RAST) system installed on the FFG-8 and analyzed the risks involved to flight operation personnel. The following tasks were required of the crew: attach a hauldown cable to the helicopter while it hovered above the deck, prepare helicopters for transit to the ship's hangar, and perform maintenance of the aircraft while in the hangar. All tasks were performed while the ship was underway, subjecting the crew to hazardous ship motions in addition to wind and rotor downwash on the flight deck from the hovering aircraft.

Task 1 of this process, the "initial hookup of the helicopter messenger line to the RAST system"[4], proved problematic to the crew. This was because of an increased balance risk created due to large ship motions and high wind loading (on the order of 25 knots). The occurrence of loss of balance was referred to as MII.

To evaluate the severity and likelihood of occurrence of MIIs, the authors studied the ship motion time histories in 15 minute durations that incorporated a range of ship speeds, heading angles, and wave modal periods.[4] A computer simulation modeled the crew members performing Task 1 in its entirety, allowing for consideration of changes in stance and position on the flight deck.

The ship motion time-histories and crew movement model were combined to provide a method to determine MII events. The resulting estimated limit value, the lateral force estimator (LFE), was a combination of earth-referenced lateral acceleration and ship-referenced

lateral acceleration due to ship roll. A MII was expected to occur when the LFE exceeded a pre-determined value called the tipping coefficient. The MII calculation did not take into account a crew member's ability to avoid stumbling.

1.1.2 Applebee-Baitis Method

At NSWCCD[1], Terrence Applebee and Eric Baitis further developed the MII calculation method for application in the time domain. However, the method was documented but never published. Applebee and Baitis theorized that MII could be calculated directly from the vertical and transverse accelerometer measurements without taking rotational angles (i.e. roll and pitch) into account. The Applebee-Baitis (AB) method assumes that ship motions are implicitly considered in accelerometer measurements, so it is unnecessary to use rotational angles to calculate MII[2].[6]

1.1.3 Graham Method

Ross Graham introduced a general lateral force estimator (GLFE) in 1990 that allowed MII to be calculated in the frequency domain. The purpose of Graham's research was to demonstrate that using roll angle as a limiting criterion for shipboard operations did not model the degradation of operational performance over time, as sea conditions worsened. At

[1]At the time this research was performed, it was called the David Taylor Model Basin (DTMB). Today the official name is NSWCCD.

[2]An informal interview was conducted with Mr. Applebee and others involved in the development and programming of the AB Method to obtain historical and formula information because the method was not formally published.[6]

the time, a typical limiting criteria for shipboard operations was a roll angle of 4 degrees. Graham noted that shipboard operations were not limited by 4 degrees of roll, but rather by the lateral and vertical accelerations that contributed to personnel loss of balance. He acknowledged the previous efforts of Baitis, et al [4], stating that the time-domain LFE was an important step forward in the development of seakeeping criteria.[2]

Graham implemented his frequency domain method for MII calculations in the Defence Research Establishment Atlantic (DREA)[3] ship motion computer program SHIPMO (SHIP MOtions in waves) for the tasks described by Baitis, et al.[4] SHIPMO was developed at DREA to predict the six degree of freedom (DOF) motions and seakeeping qualities of a ship in unidirectional and short-crested seas. [7]. MII values were calculated for a destroyer going 20 knots in high Sea State 6, where the wave height was between 5 and 6 meters and the modal period was between 12 and 16 seconds long. A tipping coefficient was determined based on human geometry, and is described in more detail in Chapter 3. Using this formulation, changing stances and deck conditions could be investigated by adjusting the tipping coefficient, but were not examined specifically.[4]

Graham compared MII values calculated for a destroyer using the LFE described by Baitis, et al[4], and the GLFE, where the calculations were made on centerline at the same height as the vertical center of gravity (VCG). A 40% increase was observed in MII incidence from the LFE to GLFE calculation at the forward perpendicular of the destroyer. Vertical accelerations had a significant influence on the results and were strongly affected by location.

[3]DREA is now Defence Research and Development Canada, Atlantic

In the case of a destroyer, he noted that the MII incidence (using the GLFE) was 2.5 times greater at the forward perpendicular than at Station 12 (two Stations aft of amidships).[2] He found decreased MII incidence with lower vertical location on the destroyer, a trend consistent for both the LFE and GLFE calculations. The influence was found to be insignificant for changes in lateral location (at the same height as the VCG).

Graham found that the greatest roll occurred in stern quartering seas, but the worst heading for MII incidence was just forward of beam. This seemed due, in part, to increased vertical accelerations at this heading and shorter encounter periods in bow seas. Because the worst condition for MII occurred at the heading that did not produce the most roll, he considered that roll was not the primary indicator of operability for deck tasks. These findings were from data taken in a short-crested Sea State 6 at 20 knots.[2]

1.1.4 Graham Method Expansion

In 1992, Graham, Baitis, and Meyers expanded on Graham's research [2] proposing that seakeeping criteria are a function of human factors limitations, not just ship motions.[5] Using Graham's GLFE calculation to predict MIIs, they focused on the occurrence of a degrading event (an undesirable event that would affect crew performance, i.e. helicopter sliding) that would effect operations of interest, They proposed that all seakeeping criteria (limiting criteria for shipboard operations) should be presented "...in terms of limits on the incidence of whatever degrading event is determined to limit the operation of interest."[5]

Personnel sliding and tipping incidence methods were described, including tipping with and without wind influence. For all methods, the tipping motion of a person was described facing forward or aft, such that tips could only occur in the port and starboard directions. The moment of inertia of the person was modelled as an ellipsoidal cylinder and the moments around each foot were taken into account. These values were omitted in references [4] and [2] due to the negligible effect the resultant terms had on the final values for MII on frigates and destroyers. However, in smaller vessels, the moments had a greater effect and were included for completeness. The incidence of MII were described in terms of both small and large longitudinal accelerations.

The researchers concluded that human factors limits, in addition to the ship motions underlying degrading events, for seakeeping criteria could be used for ship design and real time operational guidance.

1.1.5 Task Effectiveness and Recovery Time

Baitis, et al[4] determined MII limit values for four levels of risk in terms of LFE, based on the number of MII observed and how hazardous they were to the crew while performing various tasks. Graham developed MII risk levels, tabulated in Table 1.1, based on his obervations, following the idea of MII limit values. These values could only be determined through observational studies, but provided operability criterion for operations where tasks could be substantially degraded, and therefore hazardous to the crew. He proposed a one-minute deck

operation be the standard deck operation, where the tipping coefficient was 0.25. These are the standard used by the North Atlantic treaty Organization (NATO).

Table 1.1: Risk of Task Degradation

Risk Level	**MII per minute**
1. possible	0.1
2. probable	0.5
3. serious	1.5
4. severe	3.0
5. extreme	5.0

Crossland and Rich [8] built upon Graham and Colwell's [9] concept of task effectiveness to develop a way to determine critical MII risk levels, stating that it was not clear from earlier reports which method was used to determine the risk levels shown in Table 1.1. They developed a way to calculate the delay in completing a task, using the time it takes the human body to recover from a MII, which was later applied to calculating the true duration of an MII.

1.1.6 North Atlantic Treaty Organization

The *North Atlantic Treaty Organization Standardization Agreement (NATO STANAG) 4154 on Common Procedures for Seakeeping in the Ship Design Process* currently uses Graham's formulation for MII and suggested tipping coefficient as described in his 1992 paper.[5] The limiting criteria for ships is one MII per minute as given in the most recent STANAG 4154

revision.[10]

1.1.7 Experimentation

Experiments have since been performed to produce tipping coefficients outside the value initially proposed for MII. Graham's estimated tipping coefficient was based on the ratio of a person's half-stance (half the distance between their feet while standing) to their VCG.[2]

Crossland, et al (1998) performed two simulator experiments using the Large Motion Simulator (LMS) part of the Advanced Flight System at DERA (Defence, Evaluation and Research Agency) Bedford, which can operate at a 5 DOF maximum.[8] From these experiments, MII tipping coefficient values were derived for a variety of tasks, as shown in table 1.2. Task A and Task B, as defined previously, are used for the analysis in this study.

Table 1.2: Derived MII Tipping Coefficients

Task	C_T
Standing Facing Fwd/Aft (Task A)	0.270
Weapon Loading	0.200
Standing Facing Fwd/Aft with Arms Aloft	0.292
Walking on a Treadmill	0.273
Standing Facing Athwart Ships (Task B)	0.182

1.2 Motivation

Consideration of human factors has become an important safety metric due to increased efficiency and reduced manning. As per Li (2002) [11], from 1989 to 1998, 46.2% of shipboard accidents or death worldwide were reportedly due to slips and falls.

Human factors are not often adequately considered as a ship design parameter. With the trend of more efficient, smaller crews, human factors should be a high priority during the ship design phase. For this to become standard practice, human factors modelling also needs to be considered in model- and full-scale testing. During the design of a new ship, existing data and knowledge regarding human factors can then be utilized and integrated into the design.

1.3 Objectives

The objectives of this thesis are as follows:

- To compare the "Graham" and "Applebee-Baitis" time domain methods of MII calculation and determine which method should be considered more accurate.
- Examine the applicability of the methods to an unusual hull form (space capsule) and its suitability for other applications.
- Propose future work concerning methods to calculate MII.

1.4 Overview of the Thesis

Chapter 1 contains the introduction and motivation for this thesis. The history of MIIs is discussed, thesis objectives are provided, and an overview of this thesis is given.

Chapter 2 describes the test case data that was used to compare the methods. The full set of tests performed in conjunction with the test case are also described.

Chapter 3 provides the theory behind the MII calculation methods compared in this thesis. The related theory is included for completeness but was not used in the analysis.

Chapter 4 provides an analysis and discussion of the two methods.

Chapter 5 presents the results and conclusions, with proposals for future work.

Chapter 2

NASA Orion Capsule Test Data

This chapter describes the test from which the data used in this study was taken. The coordinate systems and points of interest are explained and the loading and wave conditions are discussed. Finally, the data analysis plan is described and an interpretation of the test results is provided.

2.0.1 Introduction

The data used in this study was taken from the one-quarter testing of the National Air and Space Administration (NASA) Orion Crew Exploration Vehicle (CEV); the Water Egress and Survival Trainer (WEST) test. A full-scale test, the Post-Landing Orion Recovery Test (PORT), was conducted to emulate the WEST test, but the data was not sufficient for comparison with the WEST data and so is not discussed in detail. The tests were

contracted by NASA and conducted by personnel from NSWCCD. The Orion CEV is based on the modified geometry of the Apollo capsule, but with a larger diameter of 16.5 feet and a splashdown weight 50% heavier than Apollo. Orion can hold a crew of four to six, while Apollo had a crew of three. During the Apollo era, crew egress and recovery operations were limited to sea states with a significant wave height of up to 2.5 meters or surface winds of up to 25 knots. Nearly 50% of all Apollo splashdowns resulted in capsize, also called the "Stable 2" condition. The desired orientation of the capsule (the opposite of capsize) was called the "Stable 1" condition.[12] The Orion CEV was designed to increase the sea condition limits and reduce the incidence of the Stable 2 condition after splashdown.

The author was part of the test personnel on WEST and had the opportunity to work with the PORT article used for testing in Cape Canaveral, Florida. Both tests were performed in various sea states, as defined by the Annual Sea State Occurrences in the Open Ocean North Atlantic, as documented in Lee and Bales [13] and accepted by the U.S. Navy and NATO STANAG 4154. The intent of these tests was to quantify the conditions under which it is safe to perform recovery operations.

2.0.2 Coordinate System

A right-handed coordinate system was used. The origin was located at the "top" and "front" of the vessel with the positive z-axis pointing down. The NASA coordinate system for the CEV is a modified version of this standard, with the positive x-axis pointing down as shown

in Figure 2.1. This coordinate system was used for both tests.

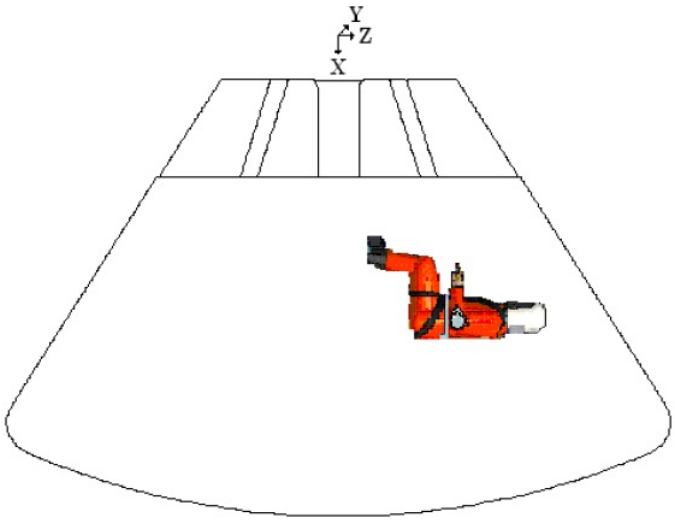

Figure 2.1: NASA coordinate system of the capsule after splash-down in the Stable 1 position.[1] Illustration used with permission.

In the surface ship hydrodynamics community, ship coordinate systems are right-handed with the positive z-axis pointing up. Figure 2.2 shows the coordinate system used for the CEV, where the origin was placed at the intersection of the baseline (bottom of the heat-shield) and amidships, z-axis pointing up, x-axis pointing towards the bow, and y-axis to port.[1] All measurements and analyses were performed in this reference frame. Motion conventions in this coordinate system are described in Table 2.1.

2.0.3 Acceleration Measurements at Points of Interest

The acceleration measurements of the sensors on both PORT and WEST models were translated to points of interest (POI) to obtain motion data and perform MII analyses at those

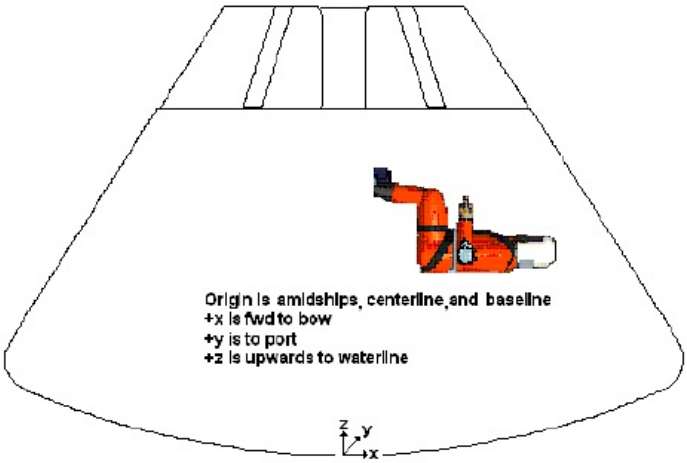

Figure 2.2: Coordinate system used for analysis of the capsule after splashdown in the Stable 1 position.[1] Illustration used with permission.

Table 2.1: Motion Convention

Axis	Translation	Rotation
x-axis	surge	roll
y-axis	sway	pitch
z-axis	heave	yaw

locations. Accelerations were translated from accelerometer measurements at the center of gravity (CG) of the capsule to ten POI (as given in Equation 3.49). In both tests, the accelerometer closest to the CG was used to calculate the translated accelerations. The POI were chosen based on assumed astronaut and rescue personnel locations during post splash down rescue operations, as specified by NASA.[1] They were used in the analysis for the WEST and PORT tests and their full scale locations are described in Table 2.2. The values are in the reference coordinate system.

Table 2.2: Acceleration Points of Interest

Locations	x	y	z
Center of Gravity (CG)	-0.13	0.01	1.18
Seat 1 Eye Point (S1)	1.30	0.39	1.61
Seat 2 Eye Point (S2)	1.30	-0.39	1.61
Seat 3 Eye Point (S3)	-0.01	0.33	1.59
Seat 4 Eye Point (S4)	-0.01	-0.33	1.59
Seat 5 Eye Point (S5)	0.94	1.06	1.64
Seat 6 Eye Point (S6)	0.94	-1.06	1.64
Side Hatch Bottom (SH)	0	1.89	1.78
Top of Docking Hatch (TH)	0	0	3.14
Forward Bay Edge 1 (FB1)	0	1.34	2.63
Forward Bay Edge 2 (FB2)	0	-1.34	2.63

*All values are full-scale meters.

2.1 Water Egress and Survival Trainer

The WEST experiment, conducted in 2008, tested the hydrodynamic performance of the CEV at one-quarter scale and consisted of a towing experiment and a hydrodynamics experiment. The main objective of the tests was to help determine the conditions in which the CEV was recoverable by search and rescue forces in various Sea States.[1]

The towing experiment determined the towing characteristics of the CEV in calm water and in Sea State 3, subsequently providing the best tow arrangement for various appendage configurations of the capsule. This experiment was conducted at NSWCCD. The data from the towing experiment is not considered in this study.

The seakeeping experiment measured the motions of the CEV, with various mass properties and appendage configurations, in Sea States 3 through 6. Testing was conducted at the Littoral Warfare Environment (LWE) at the U.S. Army's Aberdeen Proving Grounds (APG) in Aberdeen, Maryland. Analysis of the motions attempted to determine the following:

- The equilibrium position of the CEV in waves.
- The most stable ballast condition of the CEV in waves.
- The effects of aft bay flooding on stability.
- Effect of the flotation collar on the motions.
- Effect of the motions on the crew.

2.1.1 Test Conditions

For the seakeeping experiment, the model was tested in Sea States 3, 4, 5, and 6. The mean significant wave height ($H_{1/3}$) and most probable modal period (T_M) for a given sea state were utilized for these experiments and are summarized in Table 2.3.

Table 2.3: Sea State Conditions Used

Sea State	$H_{1/3}$ **(m)**		T_M **(sec)**	
	Range	**Mean**	**Range**	**Most Probable**
3	0.10 - 1.25	0.88	5.0 - 14.8	7.5
4	1.25 - 2.50	1.88	6.1 - 15.2	8.8
5	2.50 - 4.00	3.25	8.3 - 15.5	9.7
6	4.00 - 6.00	5.00	9.8 - 16.2	12.4

*All values are full-scale.

The test used two ballast conditions, with three "flooded" sub-conditions; a total of six testing conditions. The ballast conditions were "Landed Minimum" (LM) and "Abort Maximum" (AM). Respectively, they represent splashdown after a nominal end of mission and mission-abort after takeoff (heaviest) conditions. Flooded conditions tested were "Dry", "Partially Flooded" (PF), and "Fully Flooded" (FF). The latter two conditions represent damaged conditions, where seawater has entered the aft bay region of the CEV. Real-time flooding was not performed during testing. Flooding was approximated by measuring and filling the aft bay prior to testing and held constant during the testing of that condition. Fresh water was poured into the capsule through an opening made in the top near the "hatch". Threaded plugs at the bottom of the heatshield were used to drain the water. The

water was free to move around the capsule, bounded only by closed cell foam, preventing the water from going above the mid-way vertical location of the capsule. The partially flooded condition was approximated by filling the aft bay with water at 15% of its full capacity. For the fully flooded condition, the aft bay was filled to capacity. The measured flooding condition ballast weight is shown next to the model in Figure 2.3. For each of the six main conditions, a flotation collar, righting airbags, and substitute sea anchors (drogues and a depressor) were attached and tested to obtain a variety of seakeeping and motion information, should any of these appendages need to be employed on the future full scale CEV during rescue operations.[1]

Figure 2.3: WEST test article with flooding condition ballast weight.[1] Photo used with permission.

2.1.2 Setup

The one-quarter scale model was outfitted with two instruments for collecting motion data, located roughly at the center of gravity (CG) of the model. Data was translated into the NSWCCD data format, providing the accelerations, translational, and rotational values used for analysis in this thesis.

The on-board data acquisition system, provided by Microstrain, logged data continuously. All model accelerations and angular displacements were measured by a single Microstrain GX2 sensor. The data was later translated to the reference coordinate system and was filtered at 25 Hertz.

For the seakeeping portion of the test, waves were produced by 10 large plunger-type wavemakers moving in unison. A channel to produce controlled, irregular waves was created by a temporary wall (Figure 2.4) approximately 30.5 meters wide and 91.5 meters long. The wave height was measured by a TSK wave measurement device, installed 2.75 meters above the water surface. Simulated Sea States 3, 4, and 5 were very close to idealized parameters. Sea State 6 did not match as well due to limitations of the LWE. The modal period produced was shorter than the most probable modal period for the NATO-defined Sea State 6. This resulted in steeper waves, which adequately represented a lower Sea State 6, and was deemed appropriate for this experiment.

NSWCCD seakeeping testing requires ship motions in irregular waves to be reported based on a confidence level of 95%. This was achieved in a random seaway by keeping the

Figure 2.4: LWE with channel wall in place.[1] Photo used with permission.

vessel in a stationary seaway for a predetermined amount of time. The required time was based on sea state, modal period, relative wave heading, forward speed of the vessel, and the model scale ratio to achieve a statistically significant sample. The time required for each sea state was determined to be 15 minutes, representing 30 minutes of full scale time. The model took between 1 and 3 minutes to drift through the test box (Figure 2.5), so multiple passes were needed to obtain the required amount of data collection time.

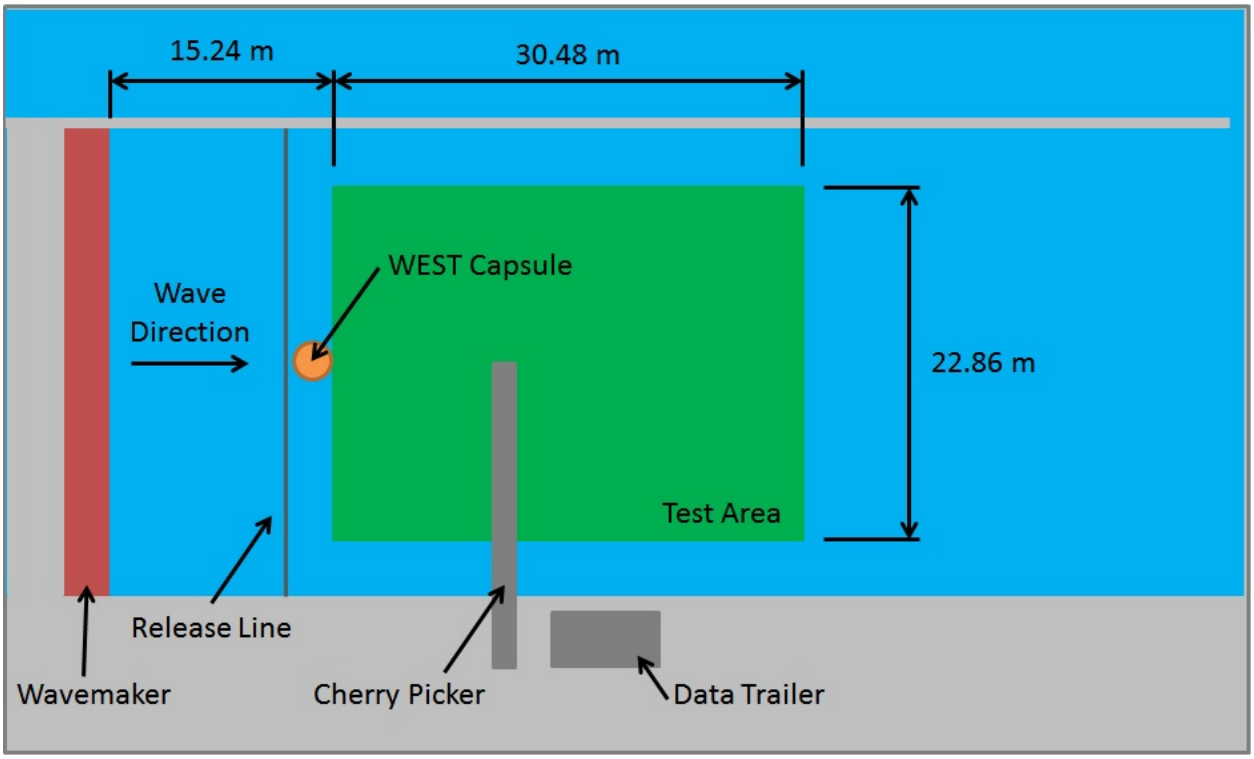

Figure 2.5: LWE test area (green).[1] Re-illustrated with permission.

2.2 Data Analyzed

Only the AM ballast condition with no appendages was utilized. All three flooding conditions are represented. The data files were organized post-test and all runs of the same condition were concatenated into one master file. PORT data was not utilized because of the lack of runs corresponding to the WEST data.

MII are calculated for a given test condition data set using the time domain methods described in Chapter 3. The tipping coefficients used are defined as Task A and Task B as tabulated in Table 1.2.

Astronauts in the full scale CEV would be sitting for the majority of the time after capsule splashdown. The MII calculated represent the recovery phase where rescue personnel would be standing outside the CEV while astronaut egress is underway and where astronauts would be sitting and standing inside the CEV.

Chapter 3

Theory

This chapter details the theory associated with the AB and Graham methods for calculating MII. The Graham method expansion regarding more detailed human-body modelling is provided. Task effectiveness and recovery time is considered and reasons why they are not used in this study are discussed. Finally, the acceleration translation theory is provided to explain how data was obtained at each point of interest.

3.1 Introduction

MII occur when the tipping ratio, R_T, exceeds the tipping coefficient, C_T, resulting in the tip inequality given in Equation 3.1.

$$R_T > C_T \tag{3.1}$$

The tipping coefficient is derived from a person's VCG and is given by

$$C_T = \frac{l}{h} \tag{3.2}$$

where l is the half-width of a person's stance and h is a person's VCG above the deck on which they are standing, as illustrated in Figure 3.1. C_T is generally estimated to be a value of 0.25, as first suggested by Graham and currently recommended by the NATO STANAG 4154.[10] Graham calculated the tipping coefficient from a stance half-width of 0.23 meters and a VCG of 0.91 meters.

3.2 Applebee-Baitis Method

The AB method is based on the assumption that ship motions are inherent in acceleration measurements such that rotational motions or rates are not needed to calculate the tipping ratio.[6] The tipping ratio for the AB method is defined as the ratio of the transverse acceleration of the vessel, a_t, to the vertical acceleration of the vessel and is given by

$$R_T = \frac{|a_t|}{a_v + g} \tag{3.3}$$

The tip inequality becomes

$$\frac{|a_t|}{a_v + g} > \frac{l}{h} \tag{3.4}$$

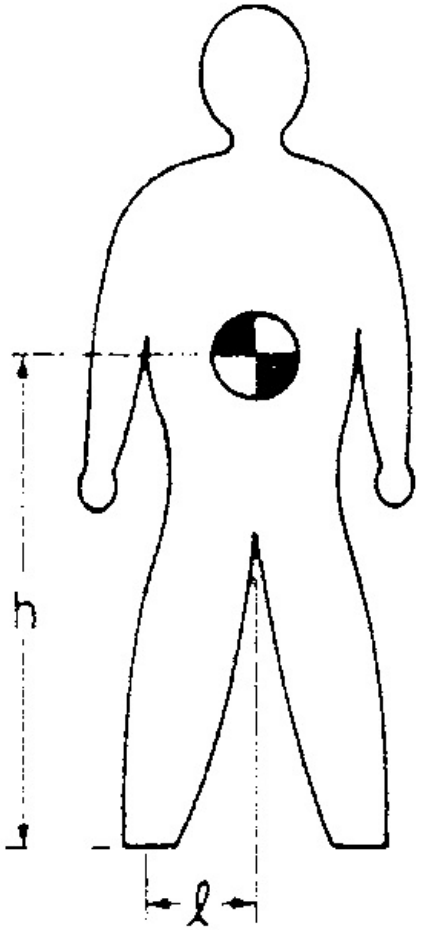

Figure 3.1: Model of a person on deck facing forward or aft.[2] Illustration used with permission.

The vertical and transverse accelerations are taken in the ship-fixed frame. To account for gravity, g is added to the vertical acceleration term in the denominator.

3.3 Graham Method

3.3.1 Independent Derivation

The Graham method equation was obtained by deriving the moments about the left and right feet using the free-body diagram (FBD) in Figure 3.2.

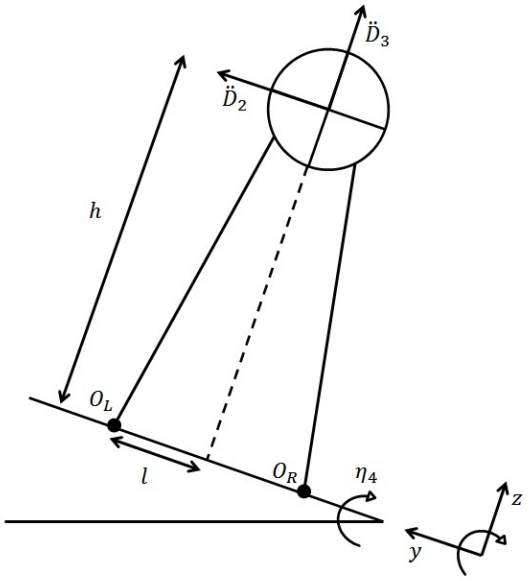

Figure 3.2: Free-Body diagram of a person facing forward rotating in the roll-axis.

The total moment about the left foot was found to be

$$\sum M_{O_L} = -\frac{1}{3}mh\ddot{\eta}_4 + mgl\cos(\eta_4) + mgh\sin(\eta_4) + ml\ddot{D}_3 + mh\ddot{D}_2 \tag{3.5}$$

where the first term is the assumed mass moment of inertia of the person.

A tip to port occurs when

$$\sum M_{O_L} < 0 \tag{3.6}$$

and small angles were assumed resulting in

$$-\frac{1}{3}h\ddot{\eta}_4 + gl + gh\eta_4 + l\ddot{D}_3 + h\ddot{D}_2 < 0 \tag{3.7}$$

The tipping coefficient, $\frac{l}{h}$, was isolated such that

$$\frac{-\frac{1}{3}h\ddot{\eta}_4 + g\eta_4 + \ddot{D}_2}{\ddot{D}_3 + g} > \frac{l}{h} \tag{3.8}$$

which, when true, results in a tip to port.

Similarly, the total moment about the right foot was found to be

$$\sum M_{O_R} = -\frac{1}{3}mh\ddot{\eta}_4 - mgl\cos(\eta_4) + mgh\sin(\eta_4) - ml\ddot{D}_3 + mh\ddot{D}_2 \tag{3.9}$$

and a tip occurs to starboard when

$$\sum M_{O_R} > 0 \tag{3.10}$$

resulting in the inequality

$$\frac{\frac{1}{3}h\ddot{\eta}_4 - g\eta_4 - \ddot{D}_2}{\ddot{D}_3 + g} > \frac{l}{h} \tag{3.11}$$

such that the tip occurs when the above equation is true.

Reducing Equations 3.8 and 3.11 resulted in

$$\frac{|-\frac{1}{3}h\ddot{\eta}_4 + \ddot{D}_2 + g\eta_4|}{\ddot{D}_3 + g} > \frac{l}{h} \tag{3.12}$$

3.3.2 Graham Derivation

Graham began his derivation by finding the forces on the person's CG in the longitudinal, lateral, and vertical directions. MII were derived assuming that longitudinal acceleration is small and wind effects were ignored.

Two coordinate systems are used for the calculations. The first is the ship inertial frame, as shown in Figure 3.3, where the origin is located at the mean position of the ship with the ability to translate with the mean velocity of the ship while maintaining a fixed orientation with respect to the free surface.[2] The heave motion displacement, $\vec{D}$, is calculated by summing the translational displacements with the cross product of the rotation measurements and the location of interest, point $\vec{P}$,

$$\vec{D} = \vec{\eta} + \vec{\xi} \times \vec{P} \tag{3.13}$$

where $\vec{\eta}$ represents the translational displacements surge, sway, and heave (η_1, η_2, η_3) and $\vec{\xi}$ represents the rotational displacements roll, pitch, and yaw (η_4, η_5, η_6). The velocities and accelerations are derived as follows,

$$\dot{\vec{D}} = \dot{\vec{\eta}} + \dot{\vec{\xi}} \times \vec{P} \tag{3.14}$$

$$\ddot{\vec{D}} = \ddot{\vec{\eta}} + \ddot{\vec{\xi}} \times \vec{P} \tag{3.15}$$

The second coordinate system, also illustrated in Figure 3.3, is the ship-fixed reference frame, where the origin and axis are fixed on the ship. This axis is used to find the forces

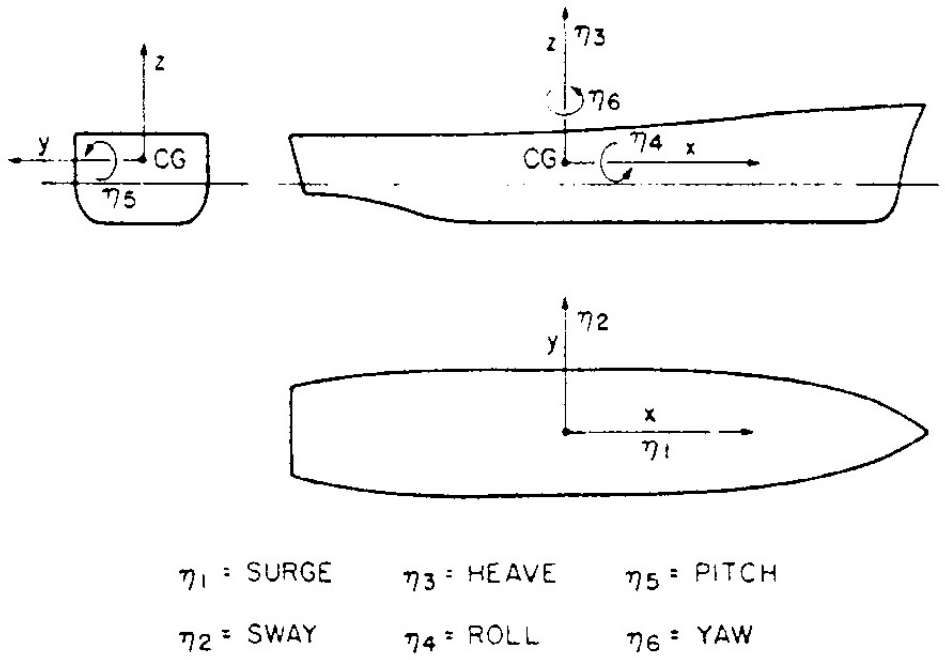

Figure 3.3: Axis system (arrows indicate sense of motion).[2] Illustration used with permission.

acting on a person (or object) in a frame of reference fixed to the ship. Coordinate transformation from the inertial frame to the ship-fixed frame, keeping only linear terms, produces the forces per unit mass at position $\vec{P}$. By keeping linear terms, it is assumed that displacements are relatively small; an appropriate approximation for the calculations used in this thesis.

It is unclear what coordinate system Graham uses for obtaining the signs for the accelerations. In Section 3.3.1, the vertical and lateral accelerations are assumed to be in line with the ship coordinate system, where up and port are positive. Graham's force Equations 3.16, 3.17, and 3.18 seem to assume accelerations are taken to be in the opposite direction, such that the acceleration terms are all negative.

The longitudinal force per unit mass, F_{Long},

$$F_{Long} = -\ddot{D}_1 + g\eta_5 \tag{3.16}$$

the lateral force per unit mass, F_{Lat},

$$F_{Lat} = -\ddot{D}_2 - g\eta_4 \tag{3.17}$$

and the vertical force per unit mass, F_{Vert},

$$F_{Vert} = -g - \ddot{D}_3 \tag{3.18}$$

Moreover, Graham assumes that the vertical force is always negative, which he forces mathematically in Equation 3.19, the condition for tipping at position $\vec{P}$ obtained by taking moments about either foot.

$$h|F_{Lat}| > -lF_{Vert} \tag{3.19}$$

or

$$|F_{Lat}| > -\frac{l}{h}F_{Vert} \tag{3.20}$$

By expanding (3.20), a MII occurs when

$$-g\eta_4 - \ddot{D}_2 - \frac{l}{h}\ddot{D}_3 > \frac{l}{h}g \tag{3.21}$$

or

$$g\eta_4 + \ddot{D}_2 - \frac{l}{h}\ddot{D}_3 > \frac{l}{h}g \tag{3.22}$$

In the case of zero vertical acceleration, $\ddot{D}_3 = 0$, these reduce to

$$|g\eta_4 + \ddot{D}_2| > \frac{l}{h}g \tag{3.23}$$

where the $g\eta_4 + \ddot{D}_2$ is defined as the LFE from reference [4].

The method was expanded by Graham, et al. [5] by modelling a person as an ellipsoidal cylinder and by looking at the moments about each foot. Supposing the person is facing forward or aft, take $\vec{P}$ to be the coordinates of the center of gravity (CG) of a person and $\vec{F}$ to be the forces acting upon their CG that results in the destabilizing moments about the feet. If the left foot is located at point $\vec{O_L}$ relative to the CG, then the moment about that foot, M_L, is

$$M_L = -\vec{O_L} \times \vec{F} \tag{3.24}$$

The same is true for the right foot. In addition to this, the ship's rotation directly induces a moment (here in the Earth-reference frame),

$$M_E = -\mathbf{I}\ddot{\vec{\xi}} \tag{3.25}$$

where $\mathbf{I}$ is the moment of inertia at the CG of the person.

The moment of inertia of a person can be estimated by the ellipsoidal cylinder with minor axis $2a$, major axis $2b$, and height $2h$, so the expanded moments of inertia are

$$\mathbf{I} = (I_X, I_Y, I_Z) = m\left(\frac{h^2}{3} + \frac{b^2}{4}, \frac{h^2}{3} + \frac{a^2}{4}, \frac{4(a^2+b^2)}{3\pi}\right) \tag{3.26}$$

and m is the mass of the person. Graham, et al[5] made the further approximation that a and b of the ellipsoid reduce to zero so

$$\mathbf{I} = (I_X, I_Y, I_Z) \approx m(\frac{h^2}{3}, \frac{h^2}{3}, 0) \tag{3.27}$$

such that the moment due to the rotation of the ship, in Earth-fixed coordinates becomes

$$M_E \approx -\frac{1}{3}mh^2(\ddot{\eta}_4, \ddot{\eta}_5, 0) \tag{3.28}$$

When transforming to the ship reference system, keeping only linear terms, the moment due to the rotation of the ship in ship-fixed coordinates, M_S, is found to be

$$M_S = M_E = -\frac{1}{3}mh^2(\ddot{\eta}_4, \ddot{\eta}_5, 0) \tag{3.29}$$

When the moments from equations 3.24 and 3.29 are combined, the total moment about the left foot becomes

$$M_{L_{total}} = -\frac{1}{3}mh^2(\ddot{\eta}_4, \ddot{\eta_5}, 0) + \vec{M_L} \tag{3.30}$$

such that a tip will occur to port when the following is true

$$M_{L_{total}} < 0 \tag{3.31}$$

Taking into account moments only in the roll-axis, a tip occurs if

$$\frac{1}{3}h\ddot{\eta}_4 - \ddot{D}_2 - g\eta_4 - \frac{l}{h}\ddot{D}_3 > \frac{l}{h}g \tag{3.32}$$

Similarly, a tip will occur to starboard if,

$$-\frac{1}{3}h\ddot{\eta}_4 + \ddot{D}_2 + g\eta_4 - \frac{l}{h}\ddot{D}_3 > \frac{l}{h}g \tag{3.33}$$

The above inequalities reduce to a tip, when considering tipping to either side, when the following is true [14],

$$\frac{|-\frac{1}{3}h\ddot{\eta}_4 + \ddot{D}_2 + g\eta_4|}{\ddot{D}_3 + g} > \frac{l}{h} \tag{3.34}$$

where the left-hand-side of the Equation 3.34 is the tipping ratio, R_T, and the right-hand-side of the equation is the tipping coefficient, C_T,

$$R_T = \frac{|-\frac{1}{3}h\ddot{\eta}_4 + \ddot{D}_2 + g\eta_4|}{\ddot{D}_3 + g} \tag{3.35}$$

$$C_T = \frac{l}{h} \tag{3.36}$$

Equation 3.34 is the same as was independently derived in Section 3.3.1. While the outcome is the same, Graham's process for obtaining it is slightly obscured by a lack of information on the assumed coordinate system of the acceleration forces.

Graham, et al. also proposed an athwart ships-facing assumption that is not reproduced here because the vessel used for this study was symmetric. This "standing facing fore or aft" equation was used by Crossland and Rich [8] when they determined various tipping coefficients (Table 1.2).

This method was also developed to calculate MIIs in the frequency domain. To most

accurately compare the Graham method to the AB method using the data available for the capsule, only the time domain equation was used. Wind-influenced calculations are not included in this thesis.

3.4 Task Effectiveness and Recovery Time

Task effectiveness, E_{TASK}, was defined by Graham and Colwell[9] as the ratio of the time required to complete a task under calm sea conditions, T_{CALM}, to the observed time to complete the same task while underway, T_{WAVES},

$$E_{TASK} = \frac{T_{CALM}}{T_{WAVES}} \tag{3.37}$$

MII experienced under calm conditions, MII_{CALM}, are

$$MII_{CALM} = T_{CALM} MII_{RATE} \tag{3.38}$$

such that the delay in completing the task in question, D_{TASK}, becomes

$$D_{TASK} = \frac{T_{CALM} MII_{RATE} D_{MII}}{60} \tag{3.39}$$

in minutes, where D_{MII} (seconds per tip) is the time taken to recover from an MII and MII_{RATE} (tips per minute) is the motion induced interruptions. While a person is experiencing an MII, the task is no longer being performed and there is now a delay in completion of the task. During this time, the person may experience more MIIs, resulting in an extra delay due to additional MIIs, given by

$$T_{WAVES} = \frac{\left(\frac{T_{CALM} MII_{RATE} D_{MII}}{60}\right) MII_{RATE} D_{MII}}{60} \tag{3.40}$$

in minutes. The extra delay can result in more MIIs, giving the infinite series,

$$T_{WAVES} = T_{CALM}\left(1 + \left(\frac{MII_{RATE} D_{MII}}{60}\right) + \left(\frac{MII_{RATE} D_{MII}}{60}\right)^2 + \left(\frac{MII_{RATE} D_{MII}}{60}\right)^3 + ...\right) \tag{3.41}$$

which converges to

$$T_{WAVES} = T_{CALM}\left(\frac{1}{1 - \frac{MII_{RATE} D_{MII}}{60}}\right) \tag{3.42}$$

if

$$\frac{MII_{RATE} D_{MII}}{60} < 1 \tag{3.43}$$

If the left-hand side of inequality (3.43) is ≥ 1, the task will not be completed. For a given number of predicted MIIs, Task Effectiveness can be determined,

$$E_{TASK} = 1 - \frac{MII_{RATE} D_{MII}}{60} \tag{3.44}$$

Alternatively, an MII criterion can be derived for a given level of acceptable task effectiveness,

$$MII_{CRIT} = \left(\frac{1 - E_{TASK}}{D_{MII}}\right) 60 \tag{3.45}$$

Crossland, et al argued that MII_{CRIT} enables MII criteria to be developed for use in the ship design assessment process such as the one outlined in the NATO STANAG 4154 [10].

The time it takes to complete a task is based on observational data and can be decomposed further by analyzing the time it takes to recover from a tip. A tip would occur for a response time equal to or greater than a specified minimum response time. A new tip would not be counted until a duration of at least the minimum recovery time had passed. This approach was not investigated for this thesis because it is important that the methods are compared on an equal basis. This is further discussed in Chapter 4.

3.5 Acceleration Translation

MII for a given time-history can be calculated by any of the described methods, for the location of the accelerometer sensor. Moreover, in order to calculate MII values at any other point, accelerations associated with that point must be available to describe the motions at that location. To do this, the accelerations from the measured sensor (location 1) must be "translated" to the POI (location 2) assuming the vessel is a rigid body. The acceleration can translate from one point to another in a rigid body because it is defined as a system of particles for which the distance between particles remain unchanged.[15] This means the position vector between points will not change as the body itself moves through space. This assumption is appropriate for smaller vessels in the ocean than larger vessels which flex with waves. Therefore, this assumption is sound for acceleration translation on the capsule. In the case of a larger vessel, flexing would need to be accounted for. During testing, this is accomplished by calculating accelerations at multiple locations on the vessel.

The acceleration value for the POI can be obtained by first finding the vector velocity by crossing the angular velocity (or rate) into the position vector,

$$v = \dot{r} = \omega \times r \tag{3.46}$$

Differentiating to get the vector acceleration gives

$$a = \dot{v} = \omega \times \dot{r} + \dot{\omega} \times r \tag{3.47}$$

or

$$a = \omega \times (\omega \times r) + \dot{\omega} \times r \tag{3.48}$$

This acceleration equation assumes that the starting location is the point of rotation. Because the measured acceleration location is not the center of rotation the equation can be generalized to go from any location to another by adding the measured acceleration such that

$$a_2 = a_1 + \dot{\omega} \times r + \omega \times (\omega \times r) \tag{3.49}$$

where a_1 is the measured acceleration value at location 1, ω are the rotational (roll, pitch, and yaw) rates, r is the vector from location 1 to location 2 and a_2 is the translated acceleration value at location 2.

Chapter 4

Analysis & Discussion

This chapter examines assumptions regarding the calculation methods and discusses why they are used. Primary analyses regarding timing between tips for both methods and a direct MII value calculation are examined. Secondary analyses compare the methods and tasks by sea state, loading condition, and vertical location and explanations are put forth. Finally, recommendations on the use of gravity and recovery time are discussed.

4.1 Assumptions for the Analysis

4.1.1 Human Vertical Center of Gravity

For MII calculation, the average human VCG is assumed to be 0.93 meters. The average human VCG was considered to be 56% of a person's height as measured from the soles of

their feet when standing with their arms at their sides. The average human height for the average American (men and women combined) between the ages of 20 and 50 was taken from the National Health Statistics Reports[16] to obtain the assumed VCG value.

Graham used a VCG value of 0.91 meters in his method for calculating MII but did not reference his choice. Upon further investigation, Graham's value was lower than the average American VCG between the ages of 20 and 50, which was 0.95 meters in a study with data from 1976 to 1980.[17] Men had an average VCG of 0.98 meters and women had an average of 0.91 meters. The same study with data from 1998 to 2002 provided an average VCG value for men and women of 0.95. The value used in this study was taken from a more recent study performed with data from 2003 - 2006. This suggests that people in the 1980s were not significantly shorter or taller than today. This implies that the 0.25 tipping coefficient value holds true today as it did when Graham first introduced the concept.

4.1.2 Vessel Shape

Although the capsule has a circular horizontal cross-section, the equations used in this thesis assume that roll is the dominant mode of motion. The axes to which all measurements are referenced is in a ship-fixed orientation. The MII calculated are for a person standing in the athwart ships position, (i.e. the roll axis runs forward to aft). The rotation of the capsule is not taken into account, so while the roll motion is mathematically assumed to be dominant, it is possible that this is not the case and at times pitch motion is dominant. For this study,

the location of all personnel in and on the capsule was assumed to be fixed with respect to the x-axis. This assumption is used to illustrate the comparison between theories.

4.1.3 Task Effectiveness & Recovery Time

Although important, the equations developed to examine task effectiveness and recovery time were not used in this study. Test subjects were not available so task completion and recovery time during calm and at sea conditions were not obtained. The method for MII calculation must be more properly defined before extra time constraints can be added to the problem.

4.2 Primary Analyses

4.2.1 Timing Analysis

The Graham and AB programs used to calculate MII scale all data to full-scale before calculating MII such that the resulting MII values are full-scale. In order to directly compare the methods, the tipping and recovery time constraints, as described in Chapter 3, were not utilized.

MII for both methods were calculated by counting the number of data points whose value exceeded the tipping coefficient (an exceedence), counting an MII only for a set of consecutive exceedences. Only one data point under the tip threshold was required to "reset"

the exceedence count for the next tip. Although this may not be the most accurate way to calculate the true number of tips, it is the best way to compare the two methods without bias.

Figure 4.1 compares the number of tip flags calculated using both methods for one sample time-history. A tip flag occurs when the value at that data point in time exceeds the tipping coefficient. As described in chapter 3, the number of tips is calculated based on the number of sequential tip flags.

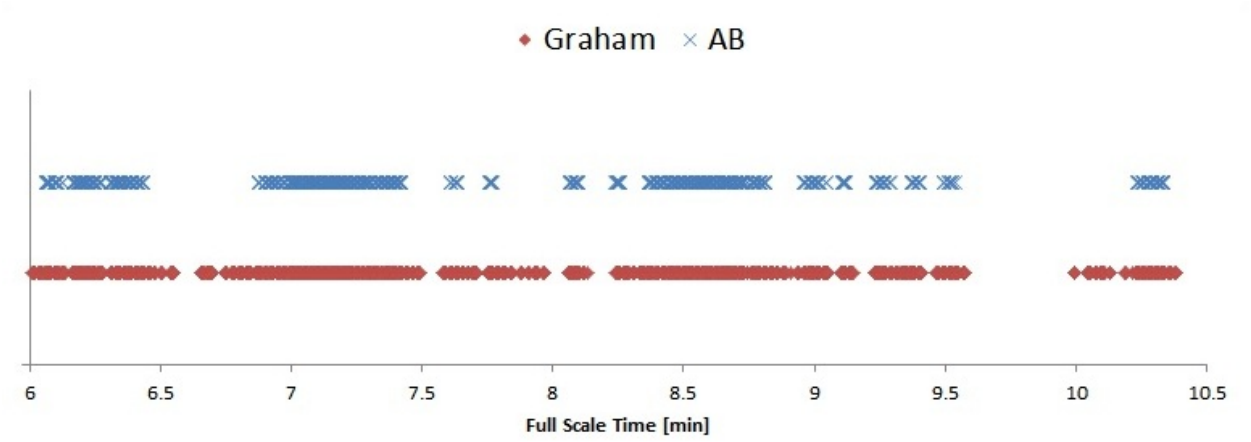

Figure 4.1: Timing analysis of both methods for the AM, FF, SS 6 case at the TH location for the WEST data.

Figure 4.1 shows that the Graham method calculates a tip before the AB method and the tip duration lasts longer. This behavior is consistant for all the capsule data. A point analysis of one occurrence was performed to further examine the behavior.

4.2.2 Point Analysis

The aforementioned behavior was decomposed by looking at individual point calculations. The AB method MII calculation, Equation 3.4, and the Graham method MII calculation, Equation 3.34, have numerators of $|a_t|$ and $|-\frac{1}{3}h\ddot{\eta}_4 + \ddot{D}_2 + g\eta_4|$, respectively. The Graham method was more complex than the AB method, so points from the WEST data set time-history are presented to more closely compare the methods. Point values are taken from the AM, FF, SS 6 case at the Top Hatch location at full-scale consecutive times of 6.096 and 6.097 minutes, presented in Table 4.1. Task B, the athwart ships case, is used in this comparison, where $C_T = 0.182$.

Table 4.1: Data from Time-History Point Analysis

Variable	Units	Point 1	Point 2
Time	$[min]$	6.096	6.097
Roll Angle	$[deg]$	4.656	5.614
Roll Acceleration	$[deg/s^2]$	-0.015	-0.018
Transverse Acceleration	$[g]$	0.145	0.162
Vertical Acceleration	$[g]$	-0.142	-0.131

From Chapter 3, the denominators of the Graham and AB equations are the same. In addition to transverse acceleration, the numerator of the Graham method includes roll angle and roll acceleration, as explained in Crossland, et al.[14] The numerator and denominator values for both methods have been calculated for the example points and are presented in Table 4.2. The Graham numerators are bigger due to the added terms, resulting in a value larger than the tipping coefficient at both times; a point exceedence. The slight difference in

numerator results in a smaller number of consecutive point exceedences for the AB method and therefore a later starting tip with a shorter duration.

Table 4.2: Method Comparison Point Analysis Results

Variable	Units	Point 1	Point 2
Graham Numerator	$[m/s^2]$	1.944	2.228
AB Numerator	$[m/s^2]$	1.420	1.591
Denominator	$[m/s^2]$	8.419	8.523
Graham Point Exceedences	–	0.231	0.265
AB Point Exceedences	–	0.169	0.189

4.2.3 Direct Comparison

Direct comparison of both methods for the WEST data shows that both sets of data follows a similar trend, but the values are quite different. The comparisons for Task B and task A, Figures 4.2 and B.1 (see Appendix B), respectively, are grouped by flooding condition across the x-axis and MII value on the y-axis. The colors represent the POI as described in Table 2.2 from Chapter 2. An initial look at the values shows a larger difference in MII at the locations farthest from the CG, the difference shrinking as the locations get closer to the CG. Figure B.1 is included in Appendix B and shows that, regardless of the tipping coefficient used, the difference between the two methods is comparable.

Initial analysis indicates that the Graham method consistently over-predicts MII with respect to the AB method, making the former a more conservative calculation. MII values

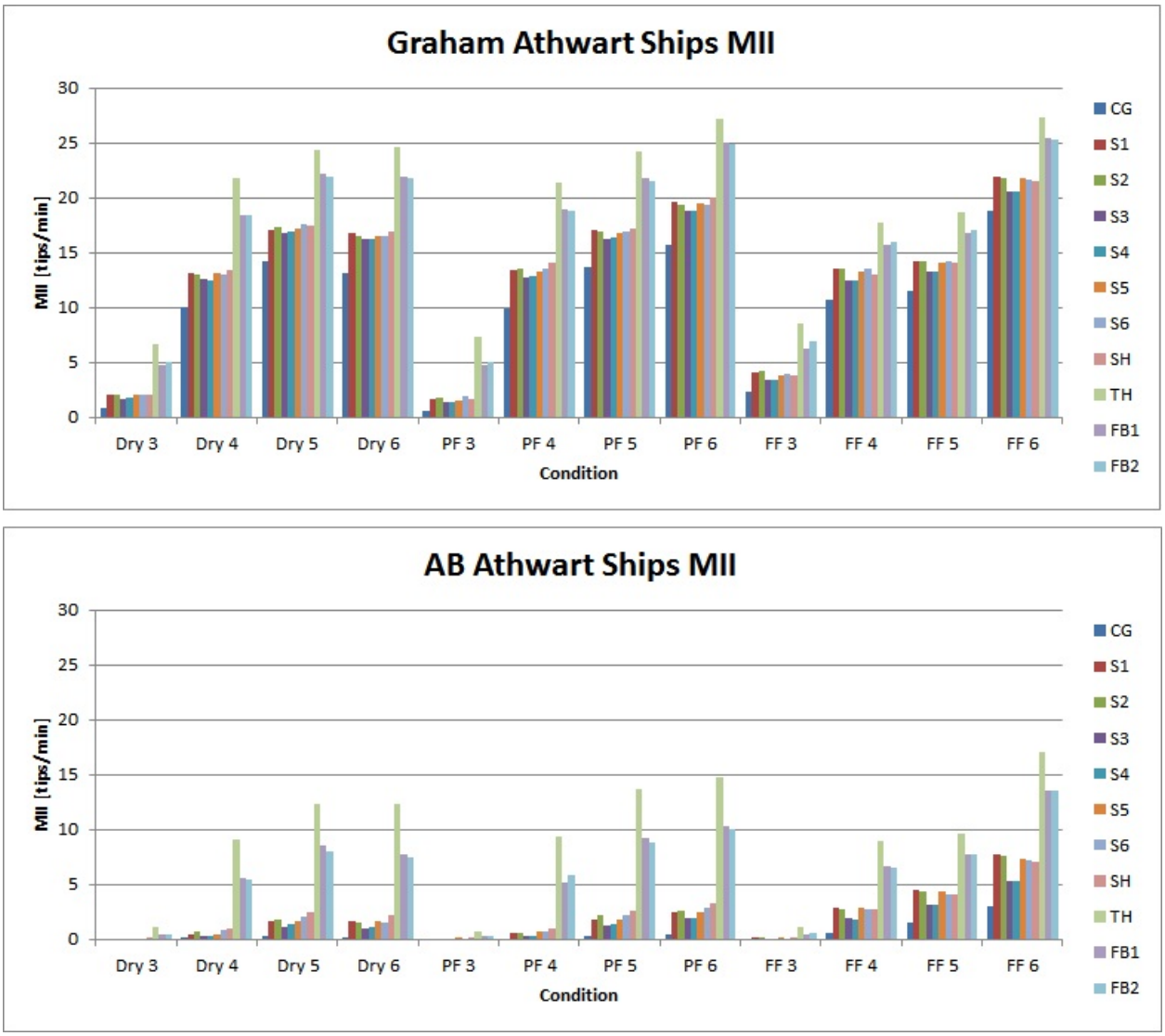

Figure 4.2: WEST MII value comparison between AB and Graham methods for Task B.

for the methods are plotted against each other in Figure 4.3 for the Dry flooding condition and it is clear that the relationship between the methods is non-linear. Conservatism is prioritized because, although one method may not be considered "right" by these findings, a more conservative estimate is preferred. Trendlines for the PF and FF flooding conditions are similar and their plots can be found in Appendix B. Due to the lack of MII occurrence, which provides an undesirable curve for analysis between the methods, Sea State 3 data is presented graphically but excluded from most further discussion. This does imply that the Orion CEV handles better in Sea State 3 than the original Apollo design, as discussed in Chapter 1.

The comparison of the two methods for both tasks over all loading conditions and sea states does not find a singular difference, ratio, or percent difference as a consistent quantifying difference. Instead, Figure 4.4 shows that as the sea state increases, the percent difference between the methods decreases. Similarly, as the CEV flooding increases, the percent difference between methods decreases, although more dramatically than just across sea states. Figure 4.5 shows that there is a non-linear relationship between task percent differences which suggests that there is a fundamental difference between the methods and how MII was calculated.

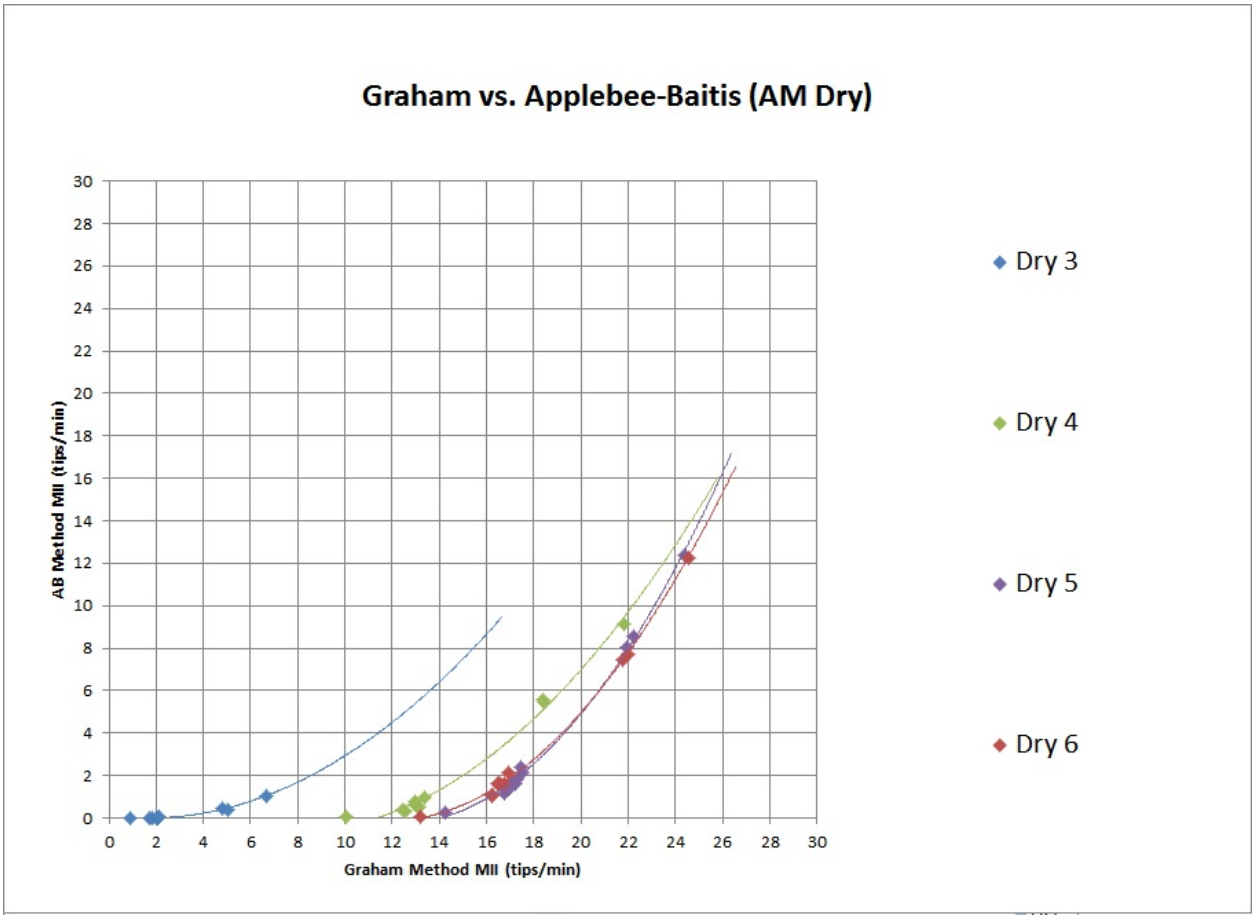

Figure 4.3: WEST MII value comparison between AB and Graham methods for Task B with trendlines.

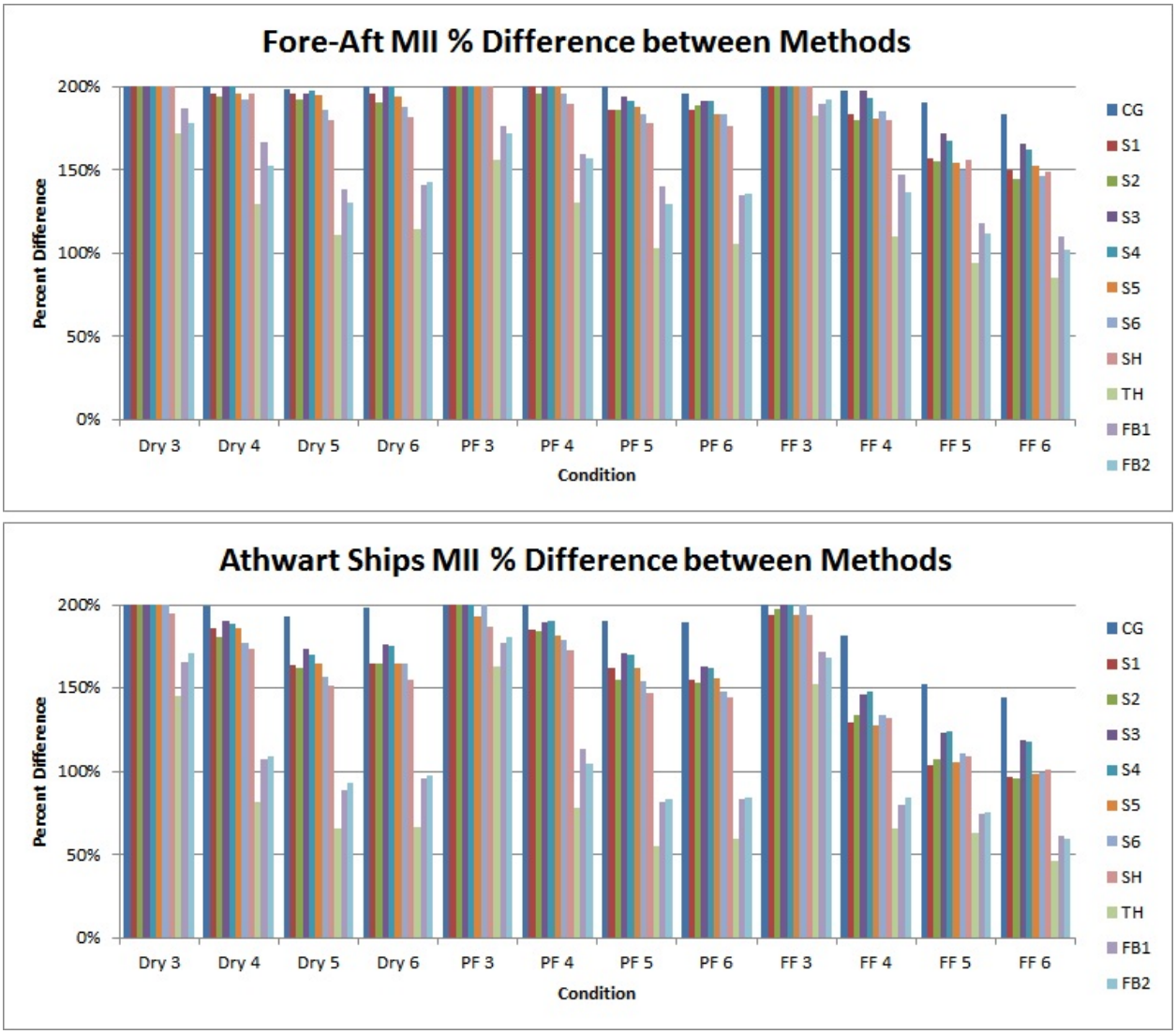

Figure 4.4: Percentage difference comparison between tasks across sea state and loading condition for Task A and Task B.

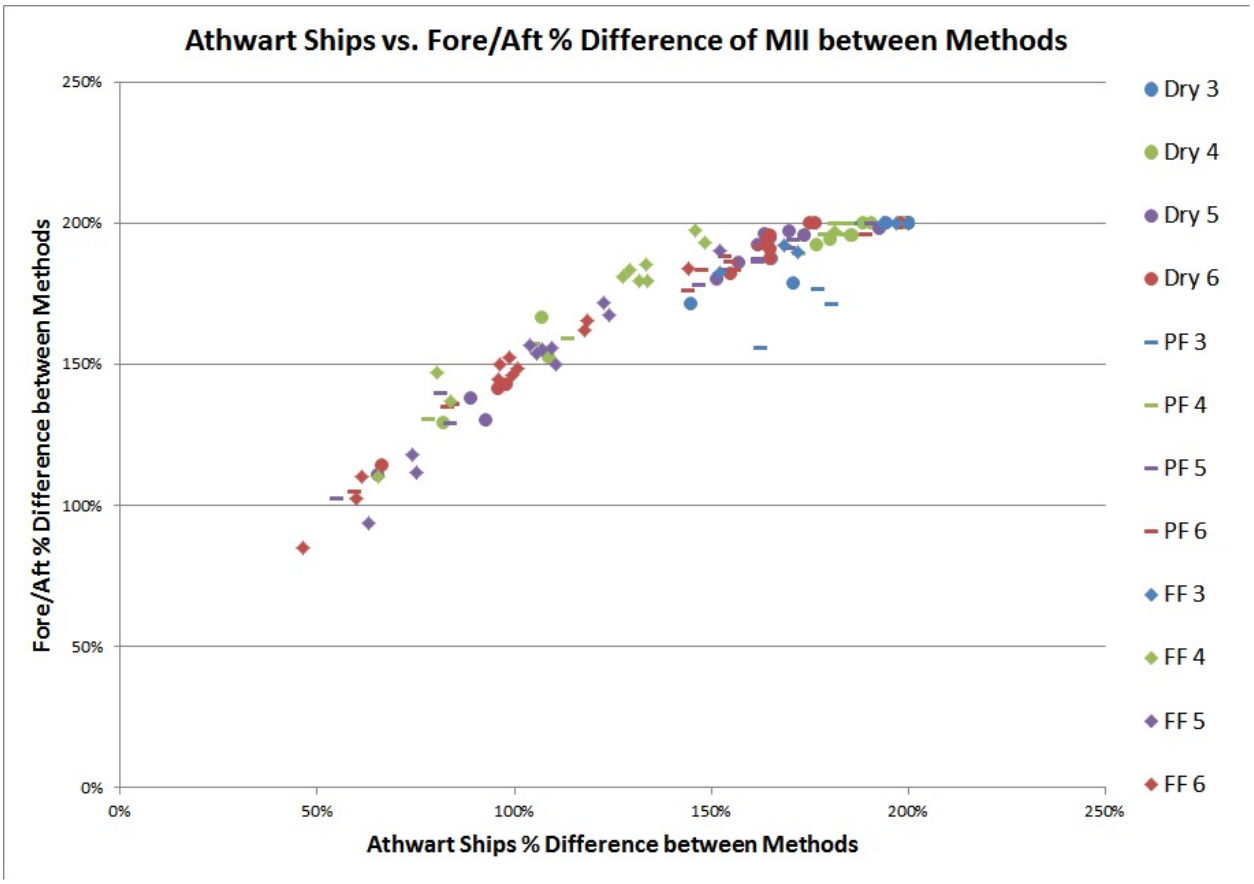

Figure 4.5: Percentage difference of methods relationship between tasks across sea state and loading condition.

4.3 Secondary Analyses

Secondary analyses were performed for a more detailed look at the differences between MII results for the two methods.

4.3.1 Methods: MII as a Function of Sea State

For both methods, MII increases as a function of sea state for the PF and FF conditions, as shown in Figure 4.6 for Task B. In the Dry condition, there is a slight decline in MII from Sea State 5 to Sea State 6. The large increase from Sea State 5 to Sea State 6 for the Fully Flooded condition can be attributed to the added weight of the full flooded aft bay. MII values increase due to the added weight and increased moment of inertia. This shows that the Graham method consistently over predicts MII as compared to the AB method, making the Graham method more conservative, as previously mentioned. The behavior is consistent for both tasks (Task A is shown in Figure B.4 in Appendix B).

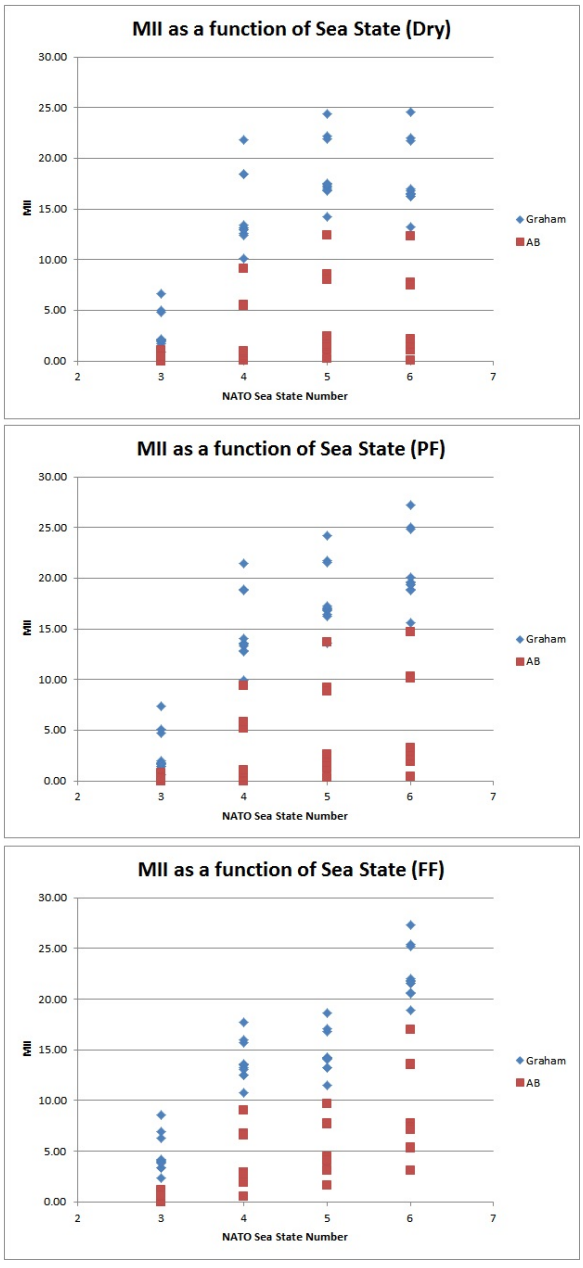

Figure 4.6: MII as a function of sea state for Task B

4.3.2 Methods: MII as a Function of Loading Condition

In Figure 4.7 and Figure B.5 (see Appendix B), conditions 1, 2, and 3 correspond to the Dry, PF, and FF conditions. Two behaviors stand out for the FF condition: higher MII values in SS3 and SS6 compared to MII values in SS4 and SS5 for FF conditions as compared to the Dry and PF conditions. In the case of higher MII values, the extra weight in the plenum could contribute to a lack of stability that could cause more MII to occur. In the case of lower MII values, the extra weight could provide more stability because of the relationship between the capsule and how the waves interact with it. Response amplitude operators (RAO) could be useful in helping determine that relationship and should be investigated further in conjunction with calculating MII.

As the sea state gets higher and as the aft bay is filled with water, the behavior is not easily predictable without more information about vessel motions due to the variable free surface effects. The hull form is not a typical ship-type, and could contribute to less confidence in the calculation, further complicated by the ability of the heat shield to fill with water.

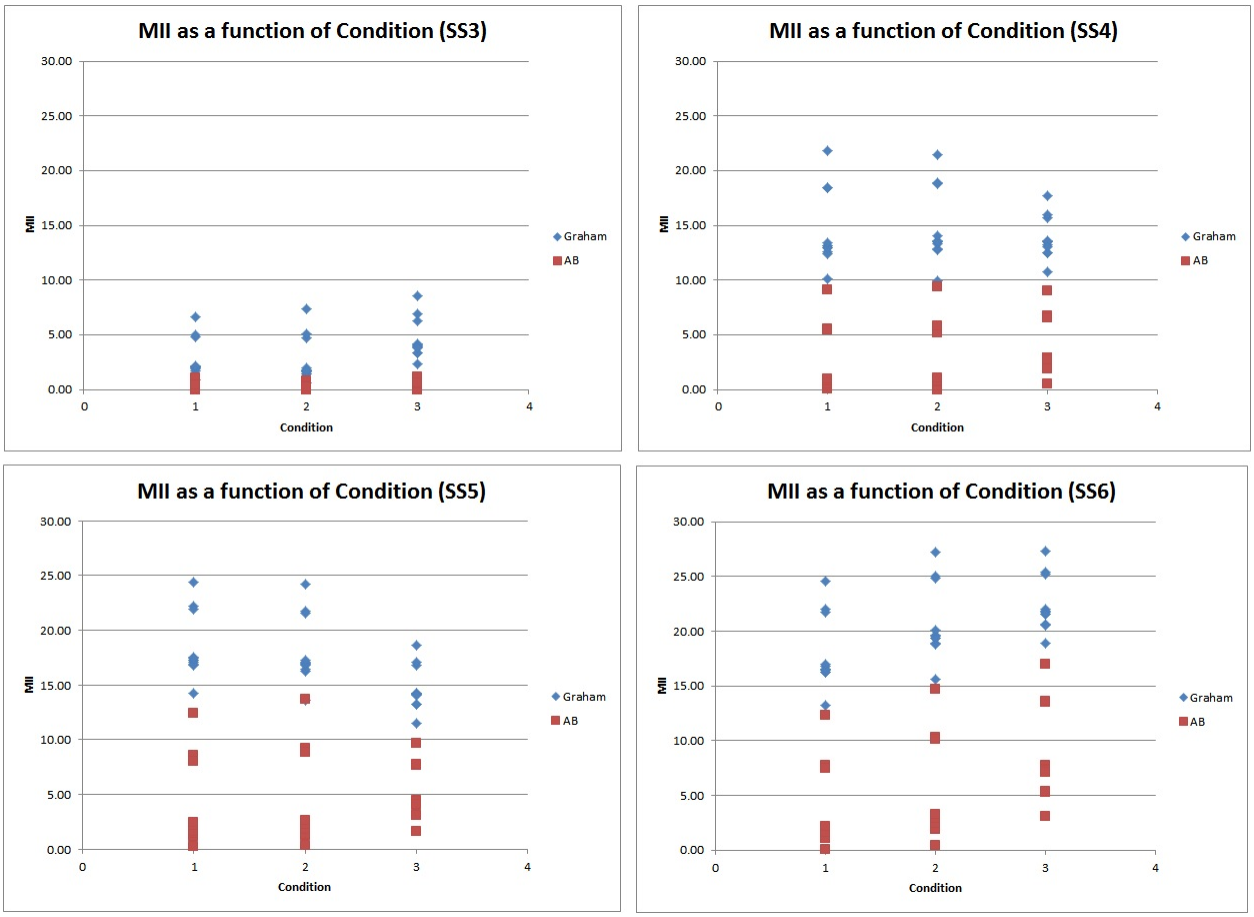

Figure 4.7: MII as a function of loading condition for Task B

4.3.3 Methods: MII as a Function of Vertical Location

The MII values were plotted against vertical location and show that the closer the location is to the CG, the fewer MIIs occur. Alternatively, the further away from the CG the location is, the more MIIs are likely to occur. In the AB method, all sea states' MII values reduce to near zero at the CG, whereas in the Graham method all MII values increase by the same order of magnitude between Sea states. In the comparison, shown in Figure 4.8, the incidence of MII reduce to near zero at the CG of the capsule for the AB method. In contrast, the difference between MII values from location to location for Sea States 4, 5, and 6 are roughly the same for the Graham method. While location behavior studies have been performed in the past, differences in sea state have not been examined. The difference between methods in location behavior should be further investigated with observational studies, as proposed in Chapter 5.

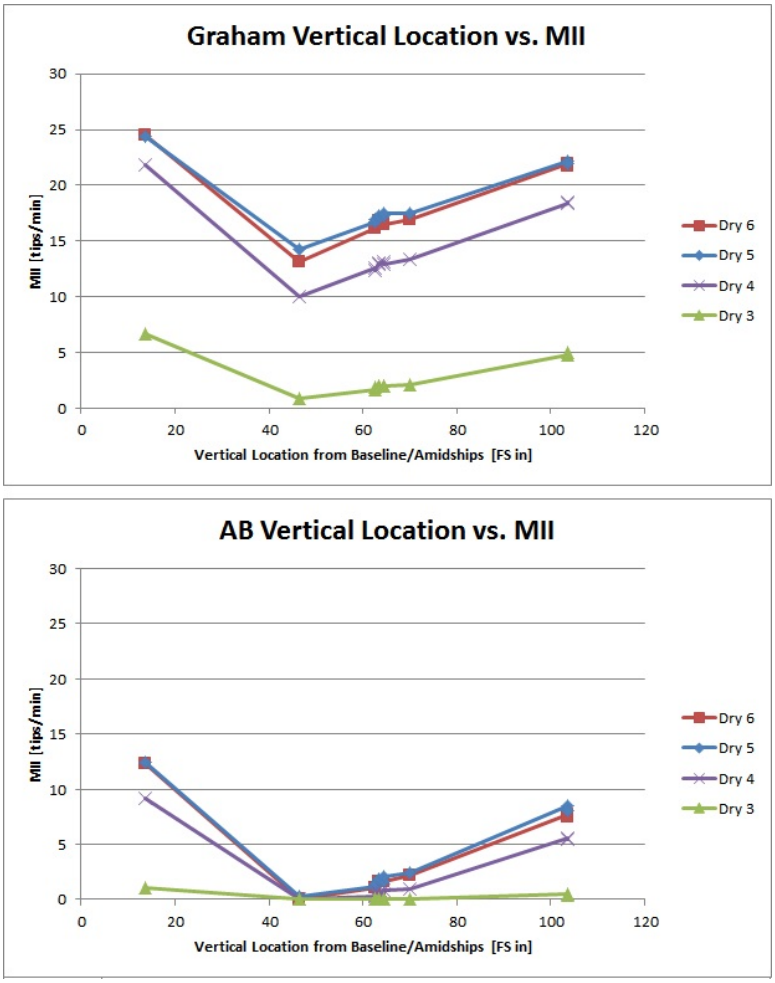

Figure 4.8: WEST MII value comparison between AB and Graham methods for Task B versus vertical location.

4.3.4 Tasks: MII as a Function of Sea State

The behaviors shown in Figure 4.9 and 4.10 show that Task A and Task B trend together for both methods, but for the AB method, the values cluster near zero. This behavior is corroborated by the zero and near-zero values found at the CG for the AB method previously.

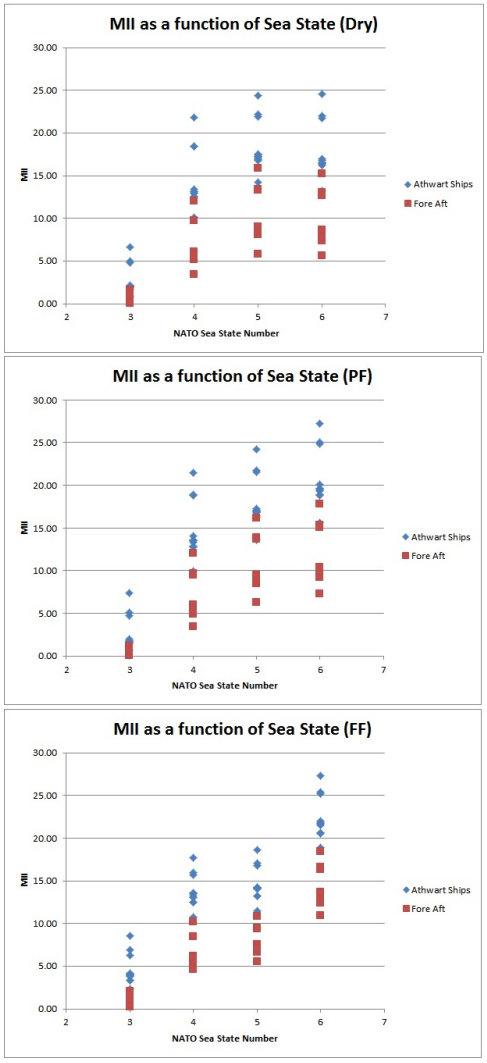

Figure 4.9: MII as a function of sea state for the Graham method

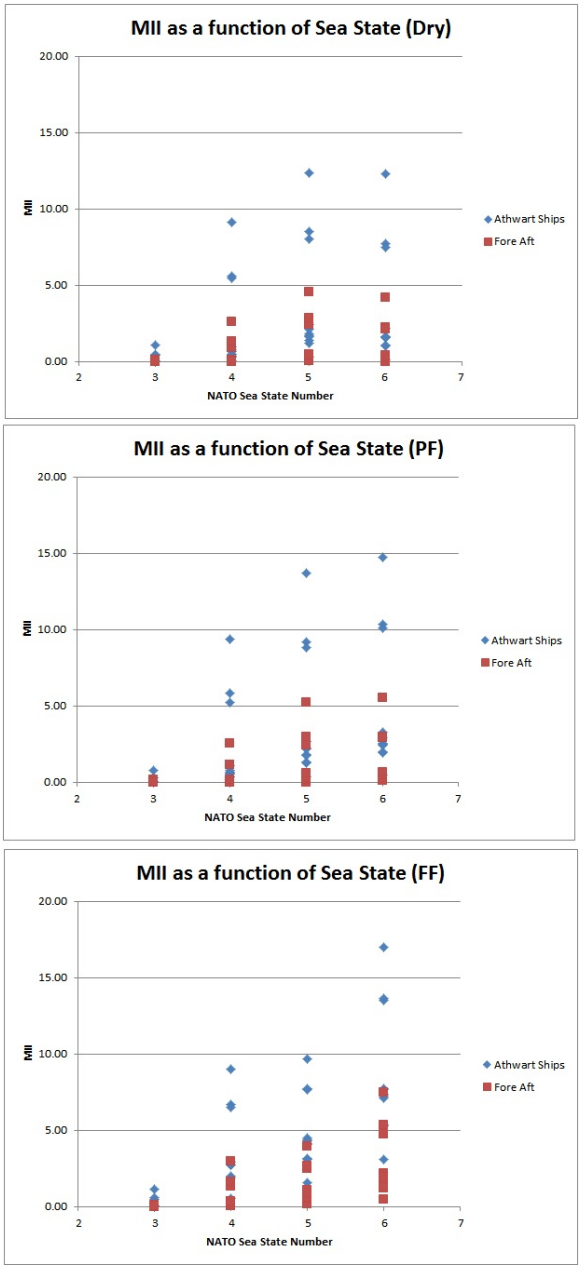

Figure 4.10: MII as a function of sea state for the AB method

4.3.5 Tasks: MII as a Function of Loading Condition

For the Graham method, the task MII values flow similarly from condition to condition. Conversely, the difference in value between tasks for the AB method is more pronounced and again, cluster near zero. This behavior mirrors the CG location dependency found for the AB method in Figure 4.8.

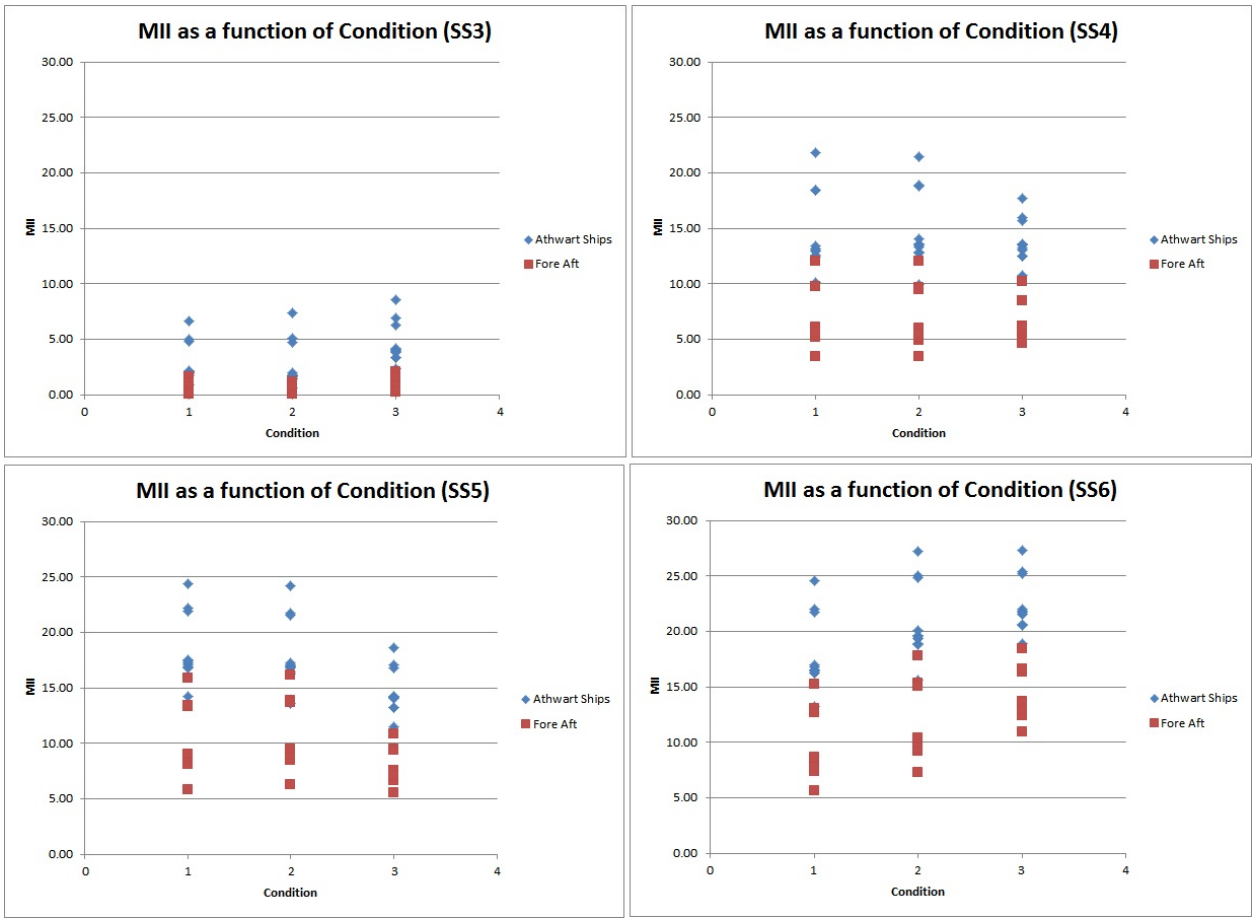

Figure 4.11: MII as a function of Loading Condition for the Graham Method

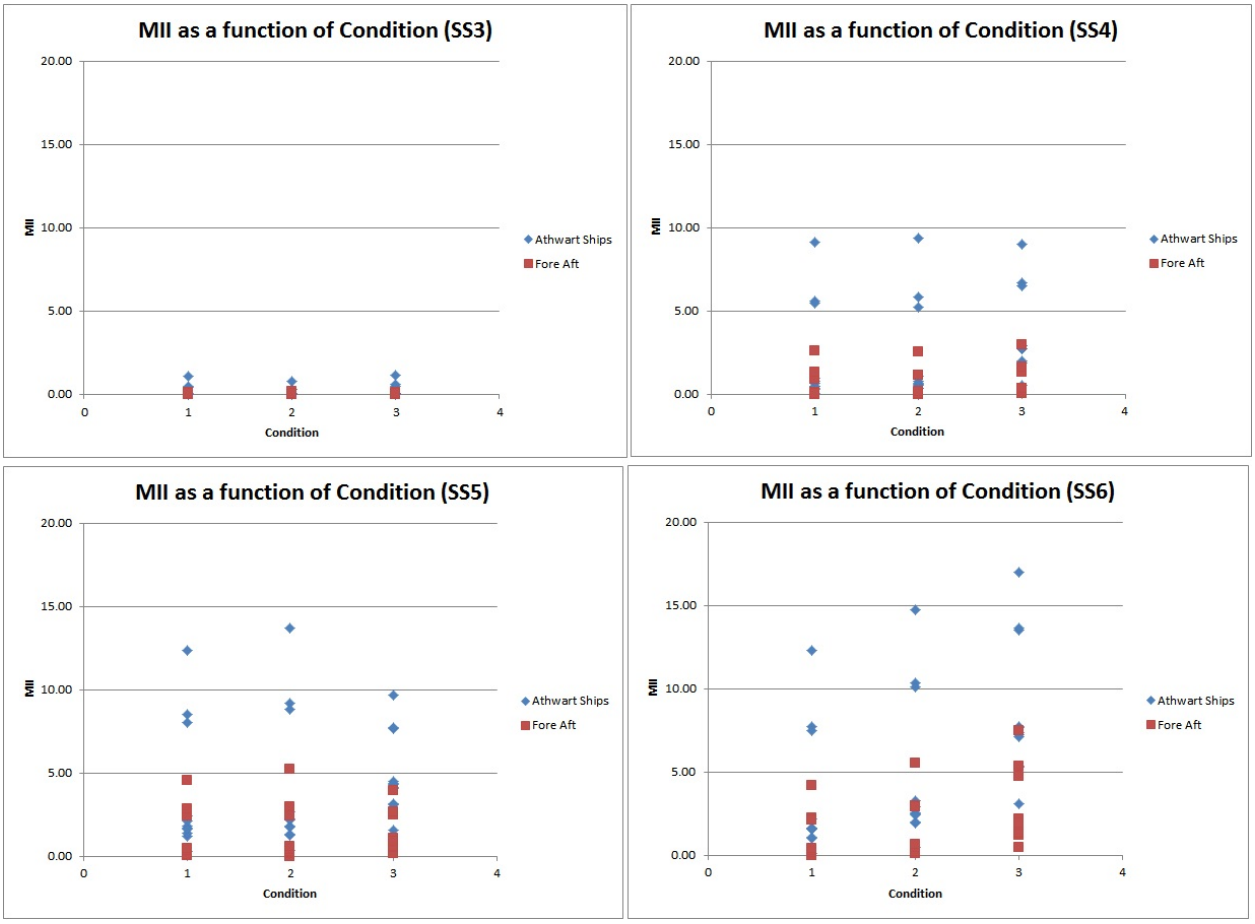

Figure 4.12: MII as a function of Loading Condition for the AB Method

4.3.6 Task Comparison by Method

Figure 4.13 and Figure 4.14 are surface plots showing the average MII task ratios and differences by sea state and loading condition. Sea State 3 is omitted because the data suggests that there are few occurrences of MII in that sea state. For the Graham Method (Figure 4.13), Task B MII values are roughly twice as high as Task A MII values. This makes sense because the equation is roll-dominant. Performing Task B (standing facing athwart ships) in a traditional hull form vessel would result in higher MII than when performing Task A (standing facing fore or aft), where a person is stabilized in the roll axis and the pitch values are low relative to roll. The ratio and difference between these tasks would be closer to 1 and 0, respectively, if the MII calculation took pitch-dominant motions into account. This is because the vessel is symmetric and it could be assumed that pitch-dominant calculations would be on the same order of magnitude as the roll-dominant calculations. This behavior is consistent for both methods.

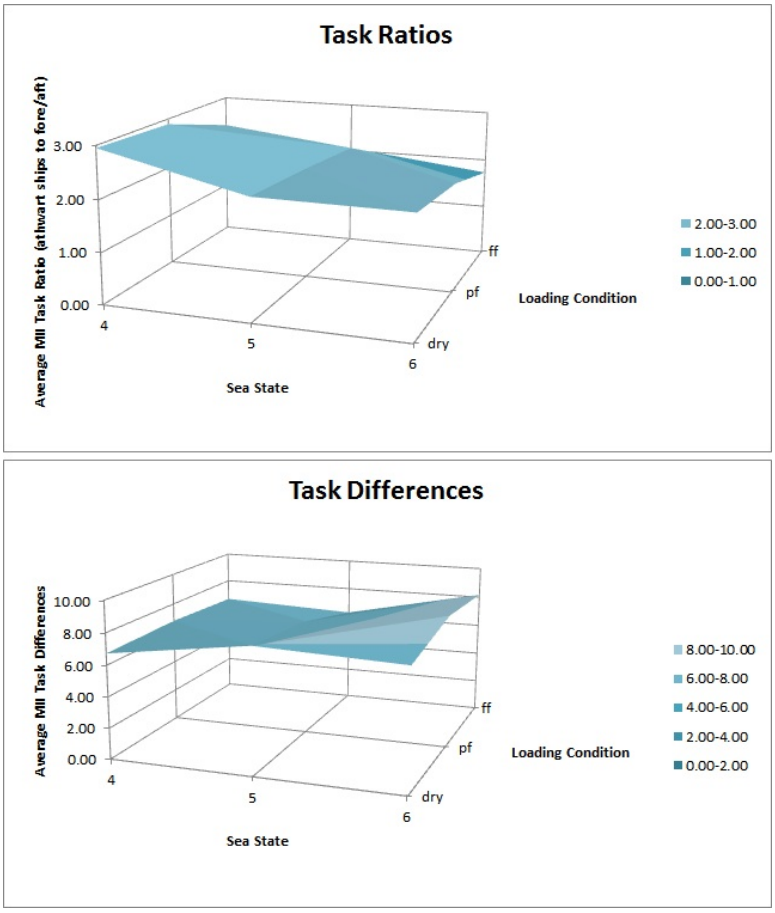

Figure 4.13: Task comparison by sea state and loading condition for the Graham method

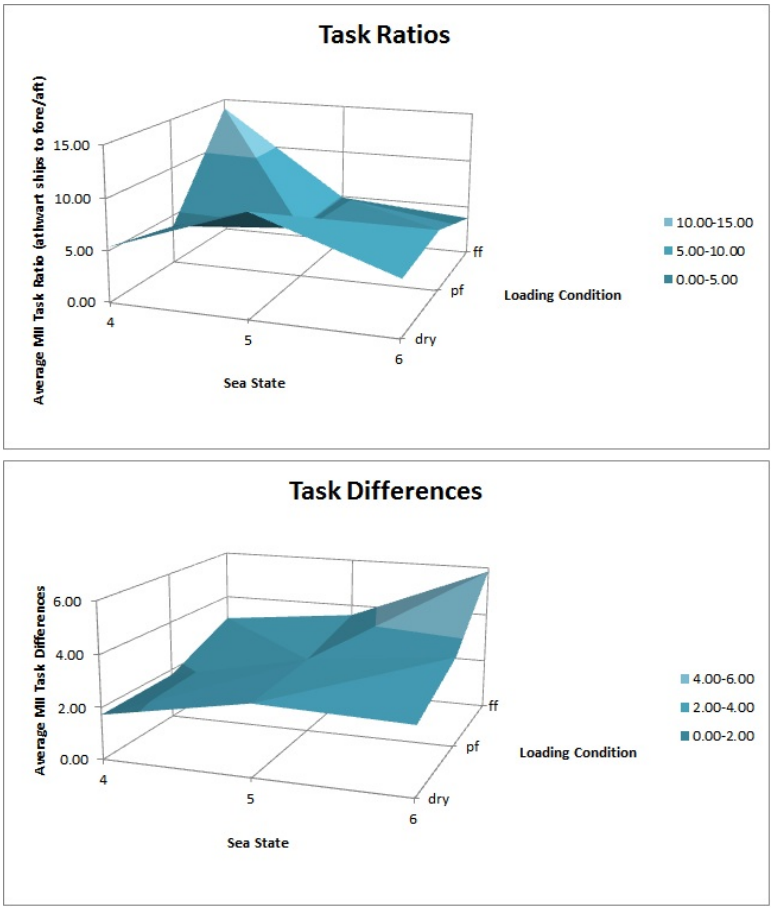

Figure 4.14: Task comparison by sea state and loading condition for the AB method

The AB method (Figure 4.14) shows more extreme differences than the Graham method and different ratio behavior. Unexpected behavior at the CG, as found in the AB method, causes one to question the AB assumption that accelerations are all that is needed to calculate MII. Furthermore, the location differences of the AB method show the values going to zero at the CG, regardless of sea state, whereas in the Graham method, the location MII values shift together by sea state. The behavior at the CG for AB method does not seem to be realistic. This finding does not appear to have been previously noted in the literature regarding MII calculation.

4.4 Recommendations

4.4.1 Location Dependency

The secondary analyses corroborate the clustering of MII values at or near zero at the CG for the AB method. This behavior, as previously noted, requires further investigation, but suggests that the assumptions made for the AB method need to be adjusted. It seems unlikely that MII would not occur at the CG for all sea conditions. Observational studies are required to determine location dependency by sea state, as proposed in Chapter 5.

4.4.2 Physics Considerations

Gravity

The AB method could be improved by using the roll and pitch components to determine how gravity will effect the resulting value due to the selected reference frame. As the equation currently exists, gravity is always pointing along the local Z-axis (the axis of vertical acceleration) instead of along the earth referenced negative z-axis (as referenced in the reference coordinate system). As a vessel rotates about the x-axis and y-axis (pitch and roll), the vessel's local z-axis rotates with it, which reduces the component of gravity at each greater angle of rotation. The current equation could be altered by using roll (or pitch depending on the vessel in question) to find the appropriate downward value of gravity acting on a person,

$$\frac{|a_T|}{a_V + g\cos\theta} \tag{4.1}$$

where θ is the roll angle.

By taking the roll (or pitch) components of gravity into account (instead of simply adding gravity to the vertical acceleration term) the resulting MII count per minute could be more accurate.

Rotation Angle Assumptions

As mentioned earlier, the hull-form data analyzed in this paper is unique in that roll and pitch motions are of the same order of magnitude. The typical assumption for both methods is only valid for vessels where the roll motion is dominant. Both methods could be expanded to take into account pitch and roll, regardless of the fact that one motion is dominant over the other or if they are on the same order of magnitude. This roll-pitch coupling could significantly alter the calculation in both methods because it then becomes a three dimensional problem. Vessels with significant roll-pitch coupling such as capsules at splashdown, surfaced manned underwater vehicles (MUV), floating platforms, etc., could benefit greatly from improved MII prediction for crew safety.

In the independent derivation of Graham's method in Section 3.3.1 of Chapter 3, small angles are assumed. However, the small angle approximation is not necessarily needed for analysis in the time domain. Graham was working in the frequency domain and could have used the assumption for linearizations required for frequency-domain analysis, applying it also to the time-domain equation. By removing the small angle assumption, the sine and cosine terms in Equations 3.5 and 3.9 would be evaluated as written. The resulting inequality for a tip to either side would be,

$$\frac{|-\frac{1}{3}h\ddot{\eta}_4 + \ddot{D}_2 + g\sin(\eta_4)|}{\ddot{D}_3 + g\cos(\eta_4)} > \frac{l}{h} \tag{4.2}$$

This form should be considered in future MII studies.

4.4.3 Recovery Time

As per Crossland, et al[8], adding recovery and tipping time would considerably alter the resulting MII for a given set of data. The author puts forth the consideration that by adding these time constraints, the comparison of the AB and Graham methods may produce a completely different set of conclusions regarding the relationship between the two time series equations, as implied in Chapter 3. A time series that gives only one tip surrounded by no tips within the time constraint in one method and multiple tips in the other would create a false comparison when looking at the component equations in question. Therefore, the recovery and tipping times were not included. This allows for a direct comparison of the two methods by looking only at their MII calculation at each time step, while not under the influence of recovery and tipping time duration. While recovery time would make MII calculation more realistic, it is important that the methods used to calculated MII are investigated and improved first and remain relatively simple to apply. Analysis of the time for tipping and recovery should be investigated in future work.

4.4.4 Scaling Analysis

Scaling analysis for the purpose of finding a scale factor for MII was performed and is included as a separate section in Appendix A.

Chapter 5

Conclusions

This chapter restates the information presented in this thesis, discusses assumptions and conclusions and proposes future work related to the study presented.

5.1 Method Comparison

Two methods of calculating MII were analyzed using data from the NASA Orion WEST experiment performed by NSWCCD in Aberdeen, Maryland. The Graham method, the typical method of choice in the ship motions human factors community, was compared to the unpublished Applebee-Baitis (AB) method, and their differences were analyzed. Recovery time was not accounted for in order to obtain a better direct comparison between the two methods.

Primary analysis found that the methods follow the same trend but ultimately produce different scalar results. A single ratio value could not be found, but in general, as the Sea State increased and as the loading condition changed from dry to flooded, the methods more closely agreed. The AB method is less likely to produce exceedences resulting in a less conservative estimate of MII. It is a simpler calculation, but consistently under-predicts MII performance as compared to the Graham method, making it a less conservative calculation and therefore, a less safe estimate of MII for a ship's crew. Because the data used were for a unique hull form, with no real datum for comparison, real world observational data of crew performance is required for validation of the two methods.

Secondary analyses found that the methods show MII dependence on vertical distance from the CG. The MII values are lower at the CG and higher as the distance from the CG increases. The AB method showed clustering near and at zero as the vertical location approached the vessel CG for all sea states. This was not the case for the Graham method. Other work researched did not provide such a result, suggesting that further investigation is needed. Observational studies in variable sea conditions should be considered to determine true MII dependency on vertical location.

The AB method could be improved by the consideration of both roll and pitch to determine the effects of gravity at each data point. The vertical component of gravity at a given roll and pitch should be considered. The Graham method could be improved using similar assumptions, as the current formulation is for typical ship geometries whose roll motions are an order of magnitude larger than their pitch motions. Such adjustments will allow for MII

calculations to be more readily applied to atypical hull-forms.

The inclusion of task effectiveness and recovery time could increase the accuracy of MII calculations. Before they are considered, the method must be more properly defined as the problem is made more complex to reduce error in the MII calculation. The more accurately the human body is modelled, the more accurate the results should be.

The conclusions, in general, point to the Graham method as the more accurate calculation for MII. It over predicts MII when compared to the AB method, making it more conservative and therefore safer for a ship's crew. The AB method's simplicity makes it attractive, but it requires further investigation with observation studies to determine its validity. The more appropriate method can truly be determined through full-scale testing with test subjects to compare actual MII to calculated. From this, a hybrid method, considering human recovery time and task effectiveness, can be produced to find the most accurate calculation for MII. Neither method is suitable for application to non-traditional hull forms because they both assume roll-dominant motions are inherent to the shape. To broaden MII calculation to their shapes, the effects of both pitch and roll should be accounted for and the methods modified. This would allow the calculation of MII to be applied to all hull forms.

5.2 Future Work

Comparisons between two methods of calculating MII shows that more work is needed to determine how to most accurately calculate MII.

Although the Orion program as an Earth to International Space Station transport has been discontinued, the Orion CEV has been re-purposed for future manned space flight to the moon and beyond. A full-scale human factors test would enable further analysis of both methods and discover recovery and tipping time constants.

Using a unique hull form for such testing and analysis would help further a more generalized approach to MII calculation and other platforms exist for the study of human factors. Model- and full-scale testing currently performed provides many opportunities to investigate real world model- and full-scale data and compare it to theory. Additionally, studies of how dominant motion RAOs compare to MII values broken out by Sea State and loading condition should be performed. If the assumptions made in Chapter 4 are correct, RAOs could be useful in predicting MII for different hull forms by examining the relationship between sea conditions and vessel motions. Task effectiveness and recovery time from a MII should be further investigated, once the appropriate method for MII calculation. In this study, task effectiveness and recovery time were dismissed to directly compare the equations, but should be utilized when studying MII in the field.

While human factors experiments have been performed, few, if any, have directly compared multiple methods of MII calculation in various scales and environmental conditions, including direct human observation. Such experiments will more accurately define motion induced interruptions for the human factors community to help design a generation of safer ships.

Bibliography

[1] T. Carrico, L. Hanyok, and R. Banko, "Quarter Scale Orion Command Module Towing and Seakeeping Experiments," Naval Surface Warfare Center, Carderock Division, 9500 MacArthur Blvd, West Bethesda MD, 20817, Tech. Rep. NSWCCD-XX-TR-2009/018, April 2009.

[2] R. Graham, "Motion-Induced Interruptions as Ship Operability Criteria," *Naval Engineers Journal*, pp. 65–71, March 1990.

[3] S. C. Stevens and M. G. Parsons, "Effects of Motions at Sea on Crew Performance: A Survey," *Marine Technology*, January 2002.

[4] A. E. Baitis, T. R. Applebee, and T. M. McNamara, "Human Factors Considerations Applied to Operations of the FFG-8 and LAMPS MK III," *Naval Engineers Journal*, pp. 191–199, May 1984.

[5] R. Graham, A. E. Baitis, and W. G. Meyers, "On the Development of Seakeeping Criteria," *Naval Engineers Journal*, pp. 262–275, May 1992.

[6] R. J. Bachman, "A Survey of Motion-Induced Human Performance Degradation," Naval Surface Warfare Center, Carderock Division, 9500 MacArthur Blvd, West Bethesda MD, 20817, Tech. Rep. NSWCCD-XX-TR-2008/050, November 2008.

[7] R. T. Schmitke and B. T. Whitten, "SHIPMO: A FORTRAN Prgram to Predict Ship Motion in Waves," DREA, Department of National Defence, Darthmouth, NS, Canada, Tech. Rep. DREA-TM-81/C, 1981.

[8] P. Crossland and K. Rich, "Validating a Model of the Effects of Ship Motion on Postural Stability," in *8th International Conference on Environmental Ergonomics*, San Diego, US, October 1997.

[9] R. Graham and J. Colwell, "Assessing the Effects of Ship Motions on Human Performance: Standard Tasks for the Naval Environment," Defence Research Establish Atlantic, Tech. Rep. NATO Working Paper AC/141 (IEG/6) SG/5-WP/15, November 1990.

[10] *NATO Standardization Agreement 4154: Common Procedures for Seakeeping in the Ship Design Process*, 3rd ed., North Atlantic Treaty Organization, November 1997.

[11] K. Li and Z. Shiping, "Maritime Professional Safety: Prevention and Legislation on Personal Injuries Onboard Ships," in *IAME Panama Conference Proceedings*. International Steering Committee, 2002.

[12] T. Caricco, "Seakeeping Performance of NASA's Orion Crew Module," in *The 29th American Towing Tank Conference Proceedings*. American Towing Tank Conference, August 2010.

[13] W. Lee and S. Bales, "Environmental Data for Design of Marine Vehicles." Ship Structures Symposium, 1984.

[14] P. Crossland, K. J. N. C. Rich, and D. Granshaw, "Validating a model for predicting motion induced interruptions to task performance using simulated motions from the FFG-8 and Type 23 frigate," Defence Evaluation and Research Agency, Tech. Rep., October 1997.

[15] J. L. Meriam and L. G. Kraige, *Engineering Mechanics, Dynamics*, 5th ed. Virginia Polytechnic Institute I& State University: John Wiley I& Sons, Inc., 2002.

[16] M. A. McDowell, C. D. Fryar, C. L. Ogden, and K. M. Flegal, "National Health Statistics Reports: Anthropometric Reference Data for Children and Adults: United States, 2003 - 2006," U.S. Department of Health and Human Services, Tech. Rep. 10, October 2008.

[17] C. L. Ogden, C. D. Fryar, M. D. Caroll, and K. M. Flegal, "Advance Data From Vital and Health Statistics: Mean Body Weight, Height, and Body Mass Index: United States, 1960 - 2002," Division of Health and Nutrition Examination Studies, Tech. Rep. 347, October 2004.

Appendix A

Scaling Analysis

MII is traditionally calculated as a full-scale value and to do this, the model-scale values are Froude scaled before being used in the equations. Currently there is no MII scaling factor.

Scaling analysis was performed to investigate scaling effects of MII calculation. WEST data was analyzed using both methods at both model- and full-scale, such that the MII values produced were in model- and full-scale, respectively. The model-scale values were then scaled, using a scaling factor $1/\sqrt{\lambda}$. The AB method values scaled as expected, producing final results that were identical between model- and full-scale. The Graham method produced a non-linear comparison of model- to full-scale results. The reason for this is unclear and requires further investigation. This appendix details the process used to obtain and analyze a MII scale factor.

A.1 Froude Scaling

The terms of the equations used to calculate MII are in a variety of units as presented in the point analysis in Table 4.1. Scaling coefficients can be determined by applying the principles of dimensional analysis and Froude scaling.

Scaling coefficients are presented in Table A.1. Values in the units column have been put into those units in the final calculation of MII (i.e. degrees have been changed to radians (rad) and g's have been changed to meters per second). From this, it can be assumed that the scale factor for MII should be $\frac{1}{\sqrt{\lambda}}$ because its units are a non-dimensional value over time.

Table A.1: Scaling Coefficients for MII calculation terms.

Variable	Units	Scaling Coefficient
MII	$[tips/min]$	$\frac{1}{\sqrt{\lambda}}$
Time	$[sec]$	$\sqrt{\lambda}$
Roll Angle	$[rad]$	1
Roll Acceleration	$[rad/s^2]$	$\frac{1}{\lambda}$
Trans Acceleration	$[m/s^2]$	1
Vert Acceleration	$[m/s^2]$	1

A.2 Results

The scaling analysis was performed by calculating MII using model- and full-scale data sets. Model-scale MII values were calculated using the measured model-scale data. The full-

scale values were calculated by scaling the measured model-scale data to full-scale before calculating the MII values. The derived MII scaling factor was applied to the model-scale MII values and directly compared to the full-scale values.

The AB method produces MII values from each scaling experiment that are identical, represented by the perfect linear relationship in Figure A.1.

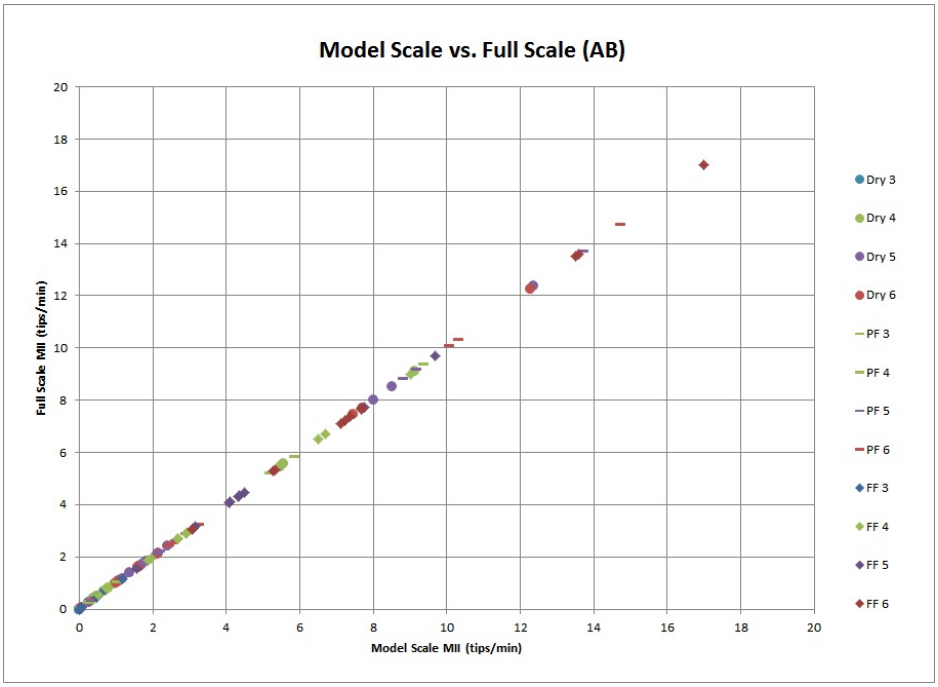

Figure A.1: Applebee Baitis scaling experiment results.

The Graham method produces MII that follow a linear trend when the model- and full-scale values are plotted against each other (Figure A.2), but scattering is apparent. This could be because the Graham method requires the scaling of time and roll acceleration as per Table A.1. All other terms are the same in full- and model-scale. The reason for the scattering requires further investigation.

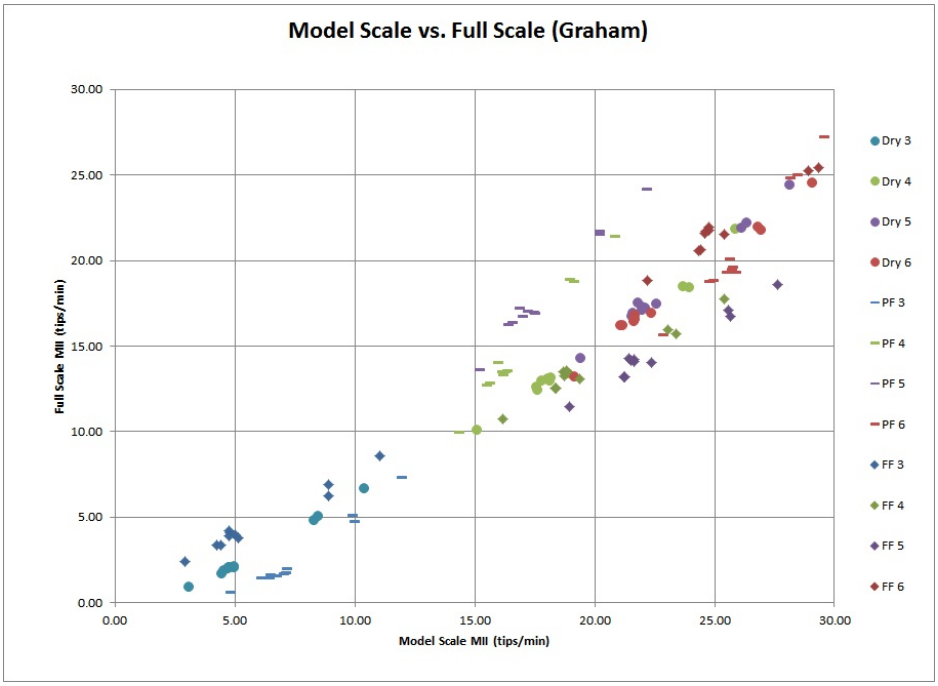

Figure A.2: Graham scaling experiment results.

Appendix B

Additional Data

This appendix contains plots that are referenced in Chapter 4 of the text.

B.1 Direct Comparison of Methods

The following plots are direct comparisons between both methods using the WEST MII values. The Bar plot represents the comparison for Task A (standing facing fore or aft) for all flooding conditions. The trendline plots represent the comparison for Task B (standing facing athwartships) for the partially flooded and fully flooded conditions.

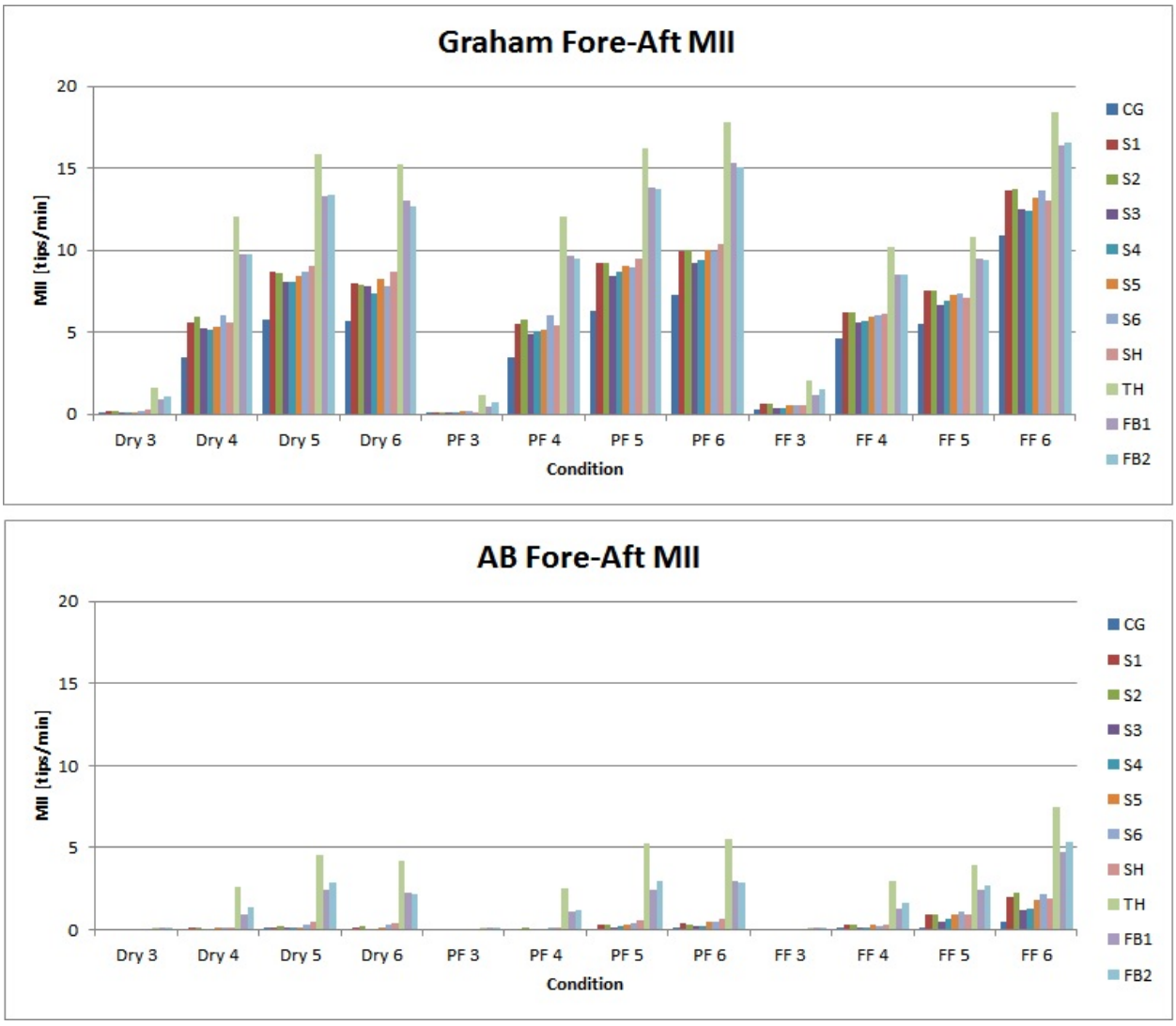

Figure B.1: WEST MII value comparison between AB and Graham methods for Task A.

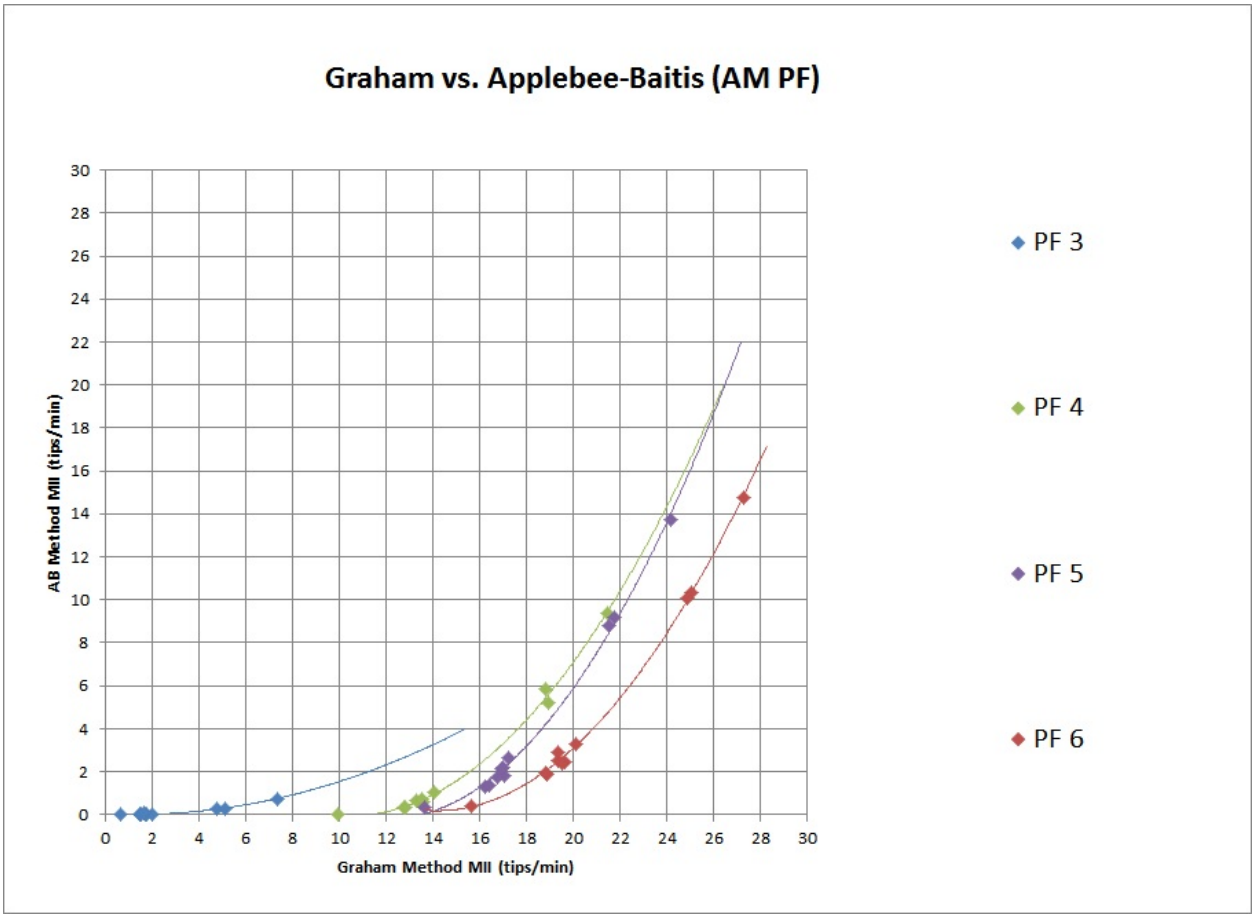

Figure B.2: WEST MII value comparison between AB and Graham methods for Task B, partially flooded condition.

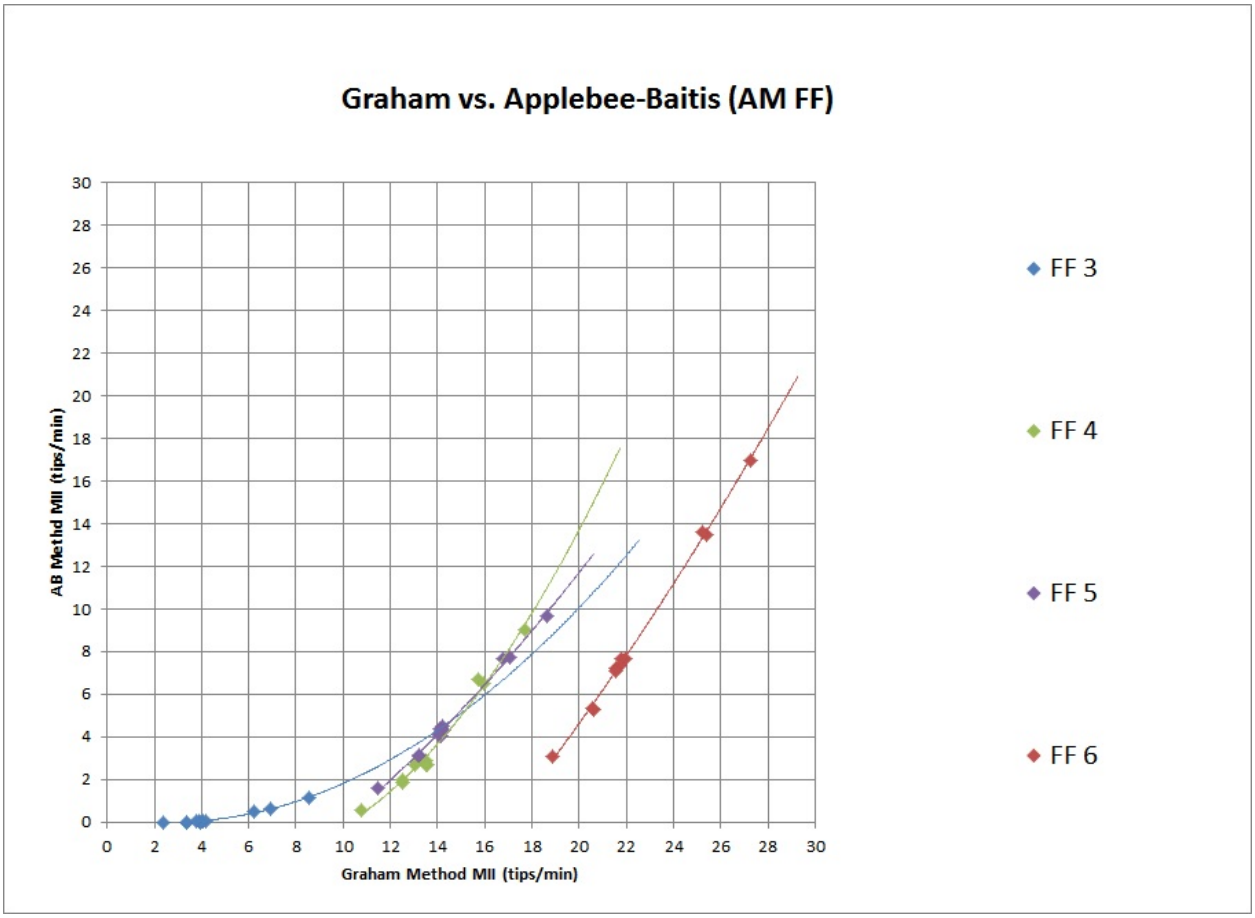

Figure B.3: WEST MII value comparison between AB and Graham methods for Task B, fully flooded condition.

B.2 MII as a Function of Multiple Variables

The following plots show MII as a function of Sea State and MII as a function of Loading Condition for Task A (Standing facing forward or aft).

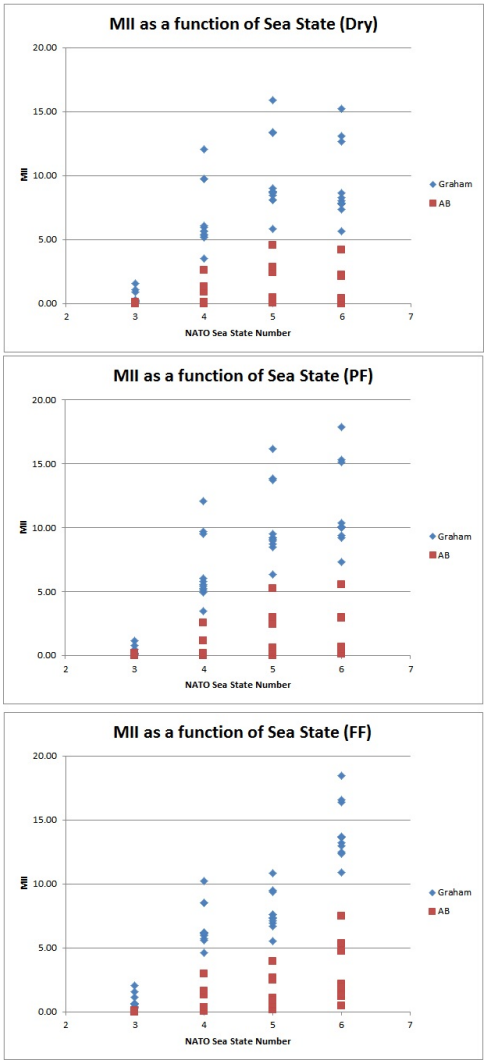

Figure B.4: MII as a function of Sea State for Task A

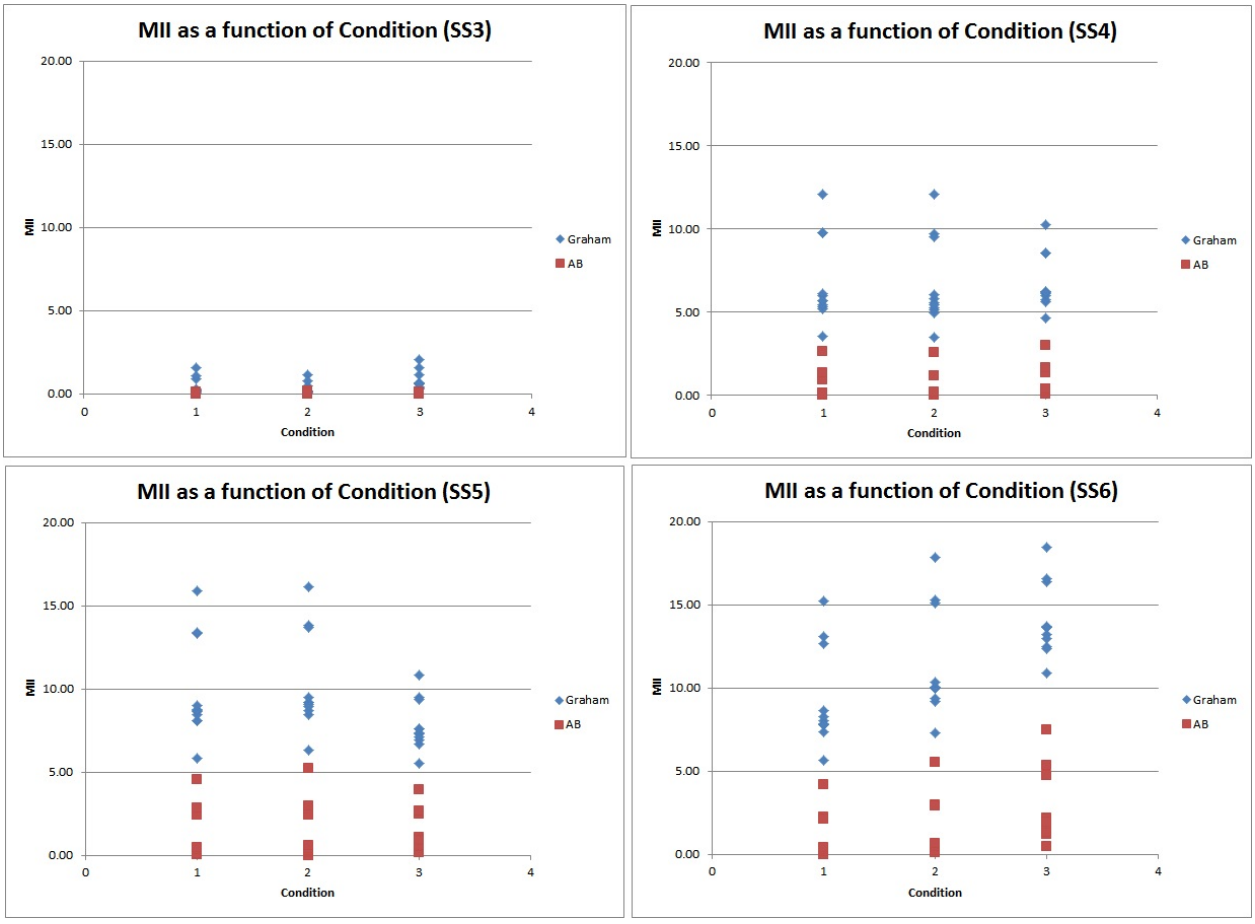

Figure B.5: MII as a function of Loading Condition for Task A